NeuroImage 284 (2023) 120459

Contents lists available at ScienceDirect

NeuroImage

journal homepage: www.elsevier.com/locate/ynimg

Modulatory effects of fMRI acquisition time of day, week and year on adolescent functional connectomes across spatial scales: Implications for inference

Linfeng Hu [a,b], Eliot S Katz [c], Catherine Stamoulis [a,d,*]

[a] Department of Pediatrics, Division of Adolescent and Young Adult Medicine, Boston Children's Hospital, Boston, MA 02115, USA
[b] Harvard School of Public Health, Department of Biostatistics, Boston, MA 02115, USA
[c] Johns Hopkins All Children's Hospital, St. Petersburg, FL 33701, USA
[d] Harvard Medical School, Department of Pediatrics, Boston, MA 02115, USA

ARTICLE INFO

Keywords:
Brain
Development
Adolescence
fMRI
Scan timing
Resting-state networks
Topological properties
Connectome

ABSTRACT

Metabolic, hormonal, autonomic and physiological rhythms may have a significant impact on cerebral hemodynamics and intrinsic brain synchronization measured with fMRI (the resting-state connectome). The impact of their characteristic time scales (hourly, circadian, seasonal), and consequently scan timing effects, on brain topology in inherently heterogeneous developing connectomes remains elusive. In a cohort of 4102 early adolescents with resting-state fMRI (median age = 120.0 months; 53.1 % females) from the Adolescent Brain Cognitive Development Study, this study investigated associations between scan time-of-day, time-of-week (school day vs weekend) and time-of-year (school year vs summer vacation) and topological properties of resting-state connectomes at multiple spatial scales. On average, participants were scanned around 2 pm, primarily during school days (60.9 %), and during the school year (74.6 %). Scan time-of-day was negatively correlated with multiple whole-brain, network-specific and regional topological properties (with the exception of a positive correlation with modularity), primarily of visual, dorsal attention, salience, frontoparietal control networks, and the basal ganglia. Being scanned during the weekend (vs a school day) was correlated with topological differences in the hippocampus and temporoparietal networks. Being scanned during the summer vacation (vs the school year) was consistently positively associated with multiple topological properties of bilateral visual, and to a lesser extent somatomotor, dorsal attention and temporoparietal networks. Time parameter interactions suggested that being scanned during the weekend and summer vacation enhanced the positive effects of being scanned in the morning. Time-of-day effects were overall small but spatially extensive, and time-of-week and time-of-year effects varied from small to large (Cohen's $f \leq 0.1$, Cohen's d<0.82, $p < 0.05$). Together, these parameters were also positively correlated with temporal fMRI signal variability but only in the left hemisphere. Finally, confounding effects of scan time parameters on relationships between connectome properties and cognitive task performance were assessed using the ABCD neurocognitive battery. Although most relationships were unaffected by scan time parameters, their combined inclusion eliminated associations between properties of visual and somatomotor networks and performance in the Matrix Reasoning and Pattern Comparison Processing Speed tasks. Thus, scan time of day, week and year may impact measurements of adolescent brain's functional circuits, and should be accounted for in studies on their associations with cognitive performance, in order to reduce the probability of incorrect inference.

1. Introduction

Over the last three decades since its discovery (Kwong, 1992, Ogawa, 1992), functional magnetic resonance imaging (fMRI) has become an indispensable tool in Neuroscience research, and has led to unprecedented discoveries on the brain's functional organization, fundamental mechanisms that facilitate information processing, and their relationships with cognition across domains (Glover, 2011;

* Correspondence author at: Department of Pediatrics, Division of Adolescent and Young Adult Medicine, Boston Children's Hospital, Boston, MA 02115, USA.
E-mail address: caterina.stamoulis@childrens.harvard.edu (C. Stamoulis).

https://doi.org/10.1016/j.neuroimage.2023.120459
Received 23 June 2023; Received in revised form 6 November 2023; Accepted 14 November 2023
Available online 15 November 2023

Bandetti, 2012; Price, 2012; Huettel, 2012). To date, almost 15,000 publications listed in PubMed are based on this modality. Beyond task-based research to elucidate the brain correlates of individual cognitive processes and system-specific functional networks, a large number of fMRI studies have also investigated the brain at rest, and large networks, including the Default-Mode Network (DMN), that are active in this state and play a ubiquitous role in cognitive function (Biswal et al., 1995; Raichle et al., 2001; Greicius et al., 2003; Fox et al., 2005; Fair et al., 2008; Van Den Heuvel et al., 2010; Calhoun et al., 2012; Smith et al., 2013, among many others). fMRI-based research continues to rapidly grow, not only as a function of technological advances in neuroimaging, but also in applications (Matthews et al., 2006; Poldrack, 2012; Calhoun et al 2014; Preti et al., 2017). fMRI can play an important role in elucidating brain correlates of neurological, neurodevelopmental, and neuropsychiatric disorders (Connelly, 1995; Rubia, 1999; Liegeois, 2004; Greicius et al., 2004; Vaidya et al., 2005; Gotman et al., 2006; Jezzard & Buxton, 2006; Stam et al., 2007; Bassett et al., 2008; Lynall et al., 2010; Chen et al., 2011; Dichter, 2012; Cortese et al., 2012; Itahashi, 2014; Hernandez et al., 2015; Walter et al., 2009, Luijten et al al, 2017 among many others). There is also growing evidence of its potential for facilitating drug discovery (Borsook, 2006; Wise & Tracey, 2006; Carmichael et al., 2018; Nathan & Bakker, 2021). Thus, given the wide utility of fMRI in basic and clinical research, and current replication crisis in the Neurosciences, it is critical to systematically investigate sources of intra- and inter-individual fMRI variability that may significantly contribute to differences between brains or snapshots of activity within the same brain, e.g., in fMRI resting-state or task-related runs, that are unrelated to the process or system of interest.

1.1. Sources of fMRI variability and confounding factors

Significant intra- and inter-individual fMRI signal variability has been reported in adults and children, and has been associated with highly variable estimates of functional and effective brain connectivity and other topological properties (Van Horn et al., 2008; Mueller et al., 2012; Baldassarre et al., 2012; Dubois & Adolphs, 2016; Liao et al., 2017; Herting et al., 2018; Foulkes & Blakemore 2018; Easson & McIntosh, 2019; Xu et al., 2019). This variability does not reflect just random BOLD fluctuations (noise), but has been attributed to the inherent heterogeneity of the brain's resting state and/or cognitive responses (Garrett et al., 2010; Grady & Garrett, 2014; Geerligs et al., 2015; Seghier & Price, 2018). fMRI signal variability often makes it difficult to reliably infer hemodynamic correlates of cognitive performance and/or topological properties of task- or resting-state networks from individual runs or sessions (McGonigle et al., 2000; Smith et al., 2005; Raemaekers et al., 2012). Although reliable connectivity measures have been reported (Aron et al., 2006; Chen et al., 2015; Abrol et al., 2017; Herting, 2018), statistical variability as a function of experimental conditions even in the resting-state (e.g., eyes open vs eyes closed) has also been reported (Patriat et al., 2013). In incompletely maturated brains, and consequently noisy circuits, intra- and inter-individual variability of fMRI signal and functional connectome estimates is likely to be higher that in adults, as a result of the individuality of neural development, and genetic, physiological, environmental, and unique experiential factors that contribute to it (McIntosh et al., 2010; Gao et al., 2014; Xu et al., 2019).

In order to separate sources of fMRI signal variability that are relevant to the scientific question of interest from unrelated contributions (Airan et al., 2016), analyses are often controlled for multiple factors, beyond demographics and/or clinical variables. These may include sleep duration, BMI, caffeine consumption, nicotine, eye fixation during the scan, respiration-related fluctuations, vascular effects, movement in the scanner, and scan length (Birn et al., 2006; Rack-Gomer & Liu, 2012; Birn et al., 2013; Murphy et al., 2013; Patriat et al., 2013; Duncan & Northoff, 2013; Arial et al., 2016; Curtis et al., 2016; Tsvetanov et al., 2021; Brooks et al., 2021; Sjuls et al., 2022; Chen et al., 2023). However, other potentially important confounders, such as scan acquisition time-of-day, chronotype (day-night phase preference) and/or seasonal effects are not usually controlled for in fMRI analyses. While information on chronotype and related factors may not be generally available, unless specifically measured, the date and time of scan are always recorded.

The circadian rhythm, sleep-wake cycle, ambient light, and physiological states, (such as alertness, arousal, sleepiness and fatigue) impact fMRI signals, estimates of functional and effective networks, and cognitive performance across the lifespan. Prior work has identified time-of-day fluctuations in multiple cognitive processes, including attention, executive function, inhibitory control and memory and their neural substrates (Anderson & Revelle, 1994; May & Hasher, 1998; Valdez et al., 2005; May et al., 2005; Schmidt et al., 2007; Gorfine & Zisapel, 2009; Marek et al., 2010; Width et al., 2011; Duyn, 2011; Park et al., 2012; Gaggioni et al., 2014; Anderson et al., 2014; Jiang et al., 2016; Facer-Childs et al., 2019; Barner et al., 2019; Smith et al., 2021; Farahani et al., 2021, 2022; Gaggero & Tommasi, 2023). Studies have also identified time-of-day and diurnal effects on functional connectivity across the brain and in individual networks, particularly the DM and sensorimotor networks, which is highest in the morning and progressively decreases throughout the day (Blautzik et al., 2013; Hodkinson et al., 2014; Orban et al., 2020). A recent study examined both functional connectivity and other topological properties of brain networks (Farahani et al., 2022). It identified increased small-worldness, assortativity as a function of time of day, higher integration of functional networks in the evening (compared to morning), regional changes in areas of the DMN, frontoparietal, attention and somatomotor networks, and high connectedness in areas of ventral attention and visual networks in the morning, and those of the somatomotor network in the evening. Another recent large-scale study based on fMRI data from the Human Connectome Project found significant time-of-day effects on the brain's hemodynamic response function but not on effective connectivity (Vaisvilaite et al., 2022), partly as a result of metabolic variations throughout the day (Shannon et al., 2013).

Beyond metabolic variations, other related factors may contribute to time-of-day effects on fMRI signals. These include sleep inertia, sleepiness and fatigue. Sleep inertia, the temporary physiological state associated with decreased alertness, cognitive performance and sensorimotor function upon awakening, has also been associated with changes in functional connectivity. In individuals who do not obtain sufficient sleep, it can linger for up to two hours after awakening (Jewett et al., 1999), and may significantly affect fMRI signals in those scanned within this period. Prior studies have reported brain-wide effects of sleep inertia, particularly loss of functional segregation between the DMN and task-positive dorsal and ventral attention, and sensorimotor networks (Vallat et al., 2019), and decreased functional connectivity in the DMN, dorsal attention, and frontoparietal networks (Chen et al., 2020). Independently of sleep inertia, sleepiness during the scan may also impact connectivity, though the direction of association may vary between regions. Prior studies have reported positive associations between sleepiness and functional connectivity the DMN, as well as visual and sensorimotor networks (Stoffers et al., 2015), but a negative association with thalamocortical resting-state functional connectivity (Killgore et al., 2015). Fatigue, which may also be correlated with the time of scan acquisition, can also impact fMRI signals. Prior studies have shown topological changes as a function of task-related (and thus short-term) fatigue (Sun et al., 2014), and the existence of a 'fatigue network', which involves the striatum, ventromedial and dorsolateral prefrontal cortices, and the anterior insula (Wylie et al., 2020). Cognitive fatigue was correlated with decreased connectivity in elements of this network, but increased connectivity between them and other posterior areas.

1.2. Limitations of prior research on fMRI timing and related effects

Most prior studies examining the impact of scan acquisition timing

on fMRI signal and connectivity variability (and resulting inter-individual differences), have focused on adults. Although brain development is inherently highly heterogeneous, few if any studies have focused on scan timing effects on youth connectomes and fMRI signals. Factors such as sleepiness, sleep inertia and fatigue, which partly correlate with the acquisition time-of-day, may have a significant impact on fMRI signals in children. Other timing parameters such as scanning during a school day vs weekend and/or school year vs summer vacation may also contribute to intra- and inter-individual variability of fMRI signals and topological properties, as the result of sleep duration or circadian phase variability. None of these time effects have been systematically investigated in children. Given that they may confound and contribute to the heterogeneity of developing connectomes, it is important to systematically investigate them and, if significant, control for them in analyses. This is particularly important in neuroimaging studies focusing on adolescence, a period of heightened neural maturation and profound metabolic, physiological, hormonal and circadian changes (Crowley et al., 2007).

1.3. Study goals

Leveraging the historically large and neurodevelopmentally heterogeneous cohort of the Adolescent Brain Cognitive Development (ABCD) study (Casey et al., 2018), this first-of-its kind (in size and focus on children) study systematically investigated potential acquisition timing correlates of resting-state fMRI signals and estimates of topological properties in early adolescents. In a cohort of 4102 youth with neuroimaging and neurocognitive testing at the ABCD baseline assessment (i.e., in pre/early adolescence), this study examined correlations between scan time-of-day and topological parameters, as well as fMRI signal fluctuations, and also compared these parameters in participants scanned during a school day vs the weekend, and those scanned during the school year vs summer vacation. It also investigated the interaction of timing parameters and their coupled associations with topological and signal parameters . The study hypothesized that time of scanning has a significant impact on signal and connectome properties, as a result of underlying metabolic and cardiovascular variations during the day, as well as physiological changes associated with sleep patterns, alertness and/or fatigue. It also hypothesized that these properties vary significantly between participants scanned during the weekend vs those scanned during the week, as a result of exogenous and endogenous factors, including social jet lag (which was, however, not assessed at the ABCD baseline), and similarly between participants scanned during the school year vs during the summer vacation, partly as a result of seasonal differences in human brain activity (Meyer et al., 2016), but also other complex and potentially interrelated factors, such as light exposure and sleep patterns.

The impact of fMRI acquisition time variables and their interactions on topological properties was examined across spatial scales of organization, from individual regions, to individual large-scale networks and the whole connectome. Measures of spontaneous signal fluctuation across each fMRI run were also analyzed. Finally, to directly assess the confounding effects of scan timing on associations between topological connectome properties and cognitive function, statistical analyses examined these associations using the ABCD neurocognitive battery with and without adjustments for scan time variables, with the ultimate goal to elucidate their effects on inference.

2. Methods

2.1. Participants

This study involves secondary analyses of publicly shared, completely anonymized data. The work described has been carried out in accordance with The Code of Ethics of the World Medical Association (Declaration of Helsinki) for studies involving human subjects. In addition, the ABCD is a multisite study that relies primarily on a central reseach protocol, reviewed and approved by the Institutional Review Board (IRB) at the University of California, San Diego. A few sites rely on the same protocol but have received approval from their local IRB (Auchter et al., 2018). In addition, the ABCD Coordinating Center has established a Bioethics and Medical Oversight advisory group for the study, to address ethical concerns associated with research findings (Clark et al., 2018). The present study was approved by the Institutional Review Board at Boston Children's Hospital. Resting-state (rs) fMRI, anthropometric, demographic, physiological, and behavioral data (release 4.0) from the baseline ABCD study cohort were analyzed. All data are publicly available through the National Institute of Mental Health Data Archive (NDA) (2023).

Participants were excluded based on diagnoses of Attention-Deficit/Hyperactivity Disorder, Autism Spectrum Disorder, and/or bipolar disorder, since prior work has reported abnormal functional connectivity in individuals with these disorders (Cherkassky et al., 2006; Monk et al., 2009; Assaf et al., 2010; Müller et al., 2011; Konrad & Eickhoff, 2010; Chase & Phillips, 2016). In addition, participants with clinical findings in their structural MRI and/or poor quality rs-fMRI data (based on quality controls set by the ABCD study and additional quality criteria set by our group) were also excluded. A sample of $n = 4102$ [1925 (46.9 %) males, 2177 (53.1 %) females] met all criteria for inclusion. Median sample age was 120.0 months (IQR = 13.0). Race and ethnicity distributions [2557 (62.34 %) white, 1480 (36.1 %) from a racial minority group, 65 (1.60 %) missing; 933 (22.8 %) Hispanic, 3120 (76.1 %) non-Hispanic, 49 (1.20 %) missing] were similar to those of the larger ABCD cohort. Sample demographic information is provided in Table 1.

2.2. Temporal measures of fMRI acquisition

Three measures associated with fMRI acquisition were investigated, and were extracted from the MRI QC Raw report: (a) *Time-of-day* (in hours), rounded to the nearest hour in which scanning began (variable in the range 8–20 in the dataset); (b) *Time-of-week,* a dichotomous variable (1 = school day, 2 = weekend); (c) *Time-of-year*, also a dichotomous variable (1 = school year, 2 = summer vacation). School year was assumed to be September 1 - June 15, and summer vacation June 16 - August 31, based on an average public school schedule for regions within 50 miles from the ABCD sites. The specific city-level public school school year schedule in areas where each ABCD study site is located is provided in Supplemental Table S1.

2.3. Additional variables

All analyses were adjusted for age, sex, family income, BMI, screen time and physical activity. In the same cohort, BMI and physical activity have been correlated with topological properties of the resting-state connectome (Brooks, 2021, 2023). In addition, propensity weights provided by the ABCD were used to adjust all analyses for sampling differences between the 21 study sites. Analyses also included race and ethnicity as dichotomous variables (1 = white, 0 = nonwhite; 1 = Hispanic, 0 = non-Hispanic). The unbalanced distribution of race and ethnicity in the ABCD study (predominantly white and non-Hispanic) limits more granular comparisons of racial and ethnic groups. BMI was calculated by multiplying weight (in lbs) by 703 and dividing by height^2 (in inches); height and weight data were extracted the ABCD Youth Anthropometrics instrument. Physical activity was measured as the number of days per week that the child was physically active for at least 60 min (this information was extracted from the ABCD Youth Risk Behavior Survey Exercise Physical Activity instrument). Screen time was calculated as total minutes per week spent on non-school-related activities (this information was extracted from the Youth Screen Time Survey).

Table 1
Sample demographic information, screen time, physical activity, and sleep length. *The 'other' racial category included participants from smaller racial groups (Alaska Native, American Indian, Native Hawaiian, Guamanian, Samoan, other Pacific Islander, Asian Indian, Chinese, Phillipino, Japanese, Korean, Vietnamese, other Asian), those who reported 'other race', and those who selected more than 2 racial groups in the ABCD study.

		N = 4102
Age (mo)	Median (IQR)	120.0 (13.0)
	Range	[107.0,133.0]
	Missing (N (%))	0 (0 %)
Sex	Female	2177 (53.07 %)
	Male	1925 (46.93 %)
	Missing (N (%))	0 (0 %)
Race	White	2557 (62.33 %)
	Black	851 (20.74 %)
	Asian	287 (7.00 %)
	Other	342 (8.34 %)
	Missing (N (%))	65 (1.59 %)
Ethnicity	Hispanic	933 (22.74 %)
	Non-Hispanic	3120 (76.06 %)
	Missing (N (%))	49 (1.20 %)
Screen Time	Median (IQR)	1050 (923.75)
	Missing (N (%))	3 (0.07 %)
BMI	Median (IQR)	17.546 (4.59)
	Missing	11 (0.27 %)
Physical activity	Median (IQR)	3 (3)
	Missing	11 (0.27 %)
Sleep length	Median (IQR)	8-9 h (2 h)
	Missing (N (%))	1 (0.024 %)
Pubertal Stage	Pre-puberty	902 (21.98 %)
	Early puberty	1260 (30.72 %)
	Mid puberty or later stage	1168 (28.48 %)
	Missing (N (%))	772 (18.82 %)
	<25,000	492 (11.99 %)
	25,000-49,999	542 (13.21 %)
	50,000-99,999	1000 (24.38 %)
	100,000-199,999	1212 (29.55 %)
	>=200,000	512 (12.48 %)
	Missing (N (%))	344 (8.39 %)
Primary Caregiver Education	Advanced degree (Master's professional (MD, JD, etc.) and doctoral degrees)	1126 (27.45 %)
	Bachelor's degree	1184 (28.87 %)
	Associate degree	457 (11.14 %)
	Some College	669 (16.31 %)
	High School/GED	379 (9.24 %)
	Did Not Graduate High school	284 (6.92 %)
	Missing (N (%))	3 (0.07 %)

2.4. Resting-state fMRI processing and connectivity estimation

2.4.1. Preprocessing

Structural MRI (T1w) and rs-fMRI data were acquired with 3.0T Siemens (n = 2508, 61.14 %), GE Medical Systems (n = 1118, 27.26 %), and Phillips Medical Systems (n = 476, 11.60 %) scanners. Repetition time (TR) for fMRI (2.4 mm isotropic) was 0.8 s. Each participant had up to four 5-min long scans. All data underwent two levels of preprocessing. First, they were initially minimally preprocessed by the dedicated Data Analysis, Informatics & Resources Center (DAIRC) of the ABCD study (Hagler et al., 2019). Preprocessing included correction for B0 distortion, motion and quality control, based on which some brains were excluded from further analysis. Then, data were also processed using the Next Generation Neural Data Analysis (NGNDA) platform Next-Generation Neural Data Analysis (NGNDA) platform (2021). Additional steps involved co-registration to structural MRI, normalization to MNI space, motion regression, initial frame removal, additional frame removal and interpolation to suppress artifacts, stopband filtering in the range 0.28–0.46 Hz to supress cardiorespiratory and other artifacts, and bandpass filtering in the range 0.01–0.25 Hz, which contains physiologically relevant BOLD signal energy (Yuen et al., 2019). These steps were followed by spatial dimensionality reduction (using the Schaefer-1000 cortical atlas (Schaefer et al., 2018), as well as the Melbourne subcortex (Tian et al., 2020) and Diedrichsen (Diedrichsen et al., 2009) cerebellar atlases) by averaging voxel time series within each atlas parcel. Additional signal denoising was then performed at the parcel level, using signal decomposition to identify and suppress contributions to the fMRI time series that are unrelated to BOLD activity. To account for signal amplitude differences associated with different scanners, fMRI signals were normalized by a brain-specific global median, to ensure that amplitudes were comparable across brains.

Additional details on fMRI processing using the NGNDA platform are described in prior publications using the same platform (Brooks et al., 2021). fMRI runs with more than 10 % of frames censored for motion (based on a displacement threshold of 0.3 mm) were excluded from further analysis. At rest, functional network connectivity is overall low, except in the DMN. Thus, the best-quality run was selected as the run with the lowest median connectivity. The number of frames censored for motion in the best-quality fMRI run from each participant was low (median percent of frames censored for motion = 1.87 %, IQR = 4.53 %). To ensure reliability of the findings, the second best-quality fMRI run was analyzed from a subset of n = 2991 participants with at least two runs of adequate quality for analysis (median percent of frames censored for motion = 1.87 %, IQR = 4.27 %). Best- and second best-quality runs are hereafter referred to as first and second runs.

2.4.2. Estimation of resting-state topological properties

Resting-state connectivity was estimated as the peak cross-correlation between each pair of fMRI parcel signals. In previous work (Brooks et al., 2021), an information theoretic approach was also used to estimate connectivity as mutual information between pairs of signals. Statistically similar patterns were obtained with both methods. Cohort-wide statistical connectivity thresholds were then calculated and the moderate outlier (median + 1.5*IQR) was empirically selected among others as the most adequate one (under the assumption that the brain at rest is overall weakly coordinated, with the exception of select networks, such as the DMN). This threshold was used to obtain binary and weighted adjacency matrices (setting values below the threshold to zero). Based on the median of nonzero correlation values in these adjacency matrices, another criterion for quality was set to eliminate fMRI runs with artifactually high connectivity across brain regions (possibly due to residual motion-related effects).

Topological network properties were calculated at three spatial levels, using binary and/or weighted adjacency matrices: the entire brain connectome, individual networks, and individual regions (network nodes). Analyzed networks included the large-scale resting-state networks delineated in Yeo (2011), as well as additional networks for individual subcortical structures, including the thalamus, amygdala, hippocampus, basal ganglia, and cerebellum. Estimated connectome- and network-level topological properties included efficiency, global clustering, median connectivity (within each network as well as between the network and the rest of the brain), modularity, network robustness (based on the natural connectivity measure, which corresponds to the average eigenvalue of the binary adjacency matrix; Wu et al., 2009), small worldness (estimated only at the connectome level) and topological stability (based on the largest eigenvalue of the adjacency matrix Restrepo & Hunt, 2007). Together, these properties describe the topological organization of the connectome (clustering, modularity, small

worldness), strength of its local and long-range connections (median intra- and inter-network connectivity), and resilience to perturbations (robustness and stability). Estimated local (node-level) topological properties included local clustering, centrality, and degree. Centrality reflects the topological importance of a node in the network, node degree measures the number of its connections, and local clustering measures local segregation, based on connections between each node's neighbors. Algorithms from the Brain Connectivity Toolbox (Rubinov and Sporns, 2010), and the NGDA platform were used to estimate these properties.

2.4.3. Estimation of fMRI signal variability

Temporal fluctuations of resting-state fMRI signals were quantified by the absolute coefficient of signal dispersion (defined as: $\frac{\sum_{i=1}^{n}|y_i-y_m|}{ny_m}$, with y_i the signal, n its length and y_m its median) averaged over the entire brain, individual hemispheres, and individual networks.

2.5. Statistical analysis

Multivariate linear regression models tested associations between the independent variables of interest, i.e., fMRI time-of-day, time-of-week, and time-of-year, and topological brain properties at the three scales (the dependent variables). Model-based statistical associations were considered significant only if the regression coefficient for the parameter of interest, model intercept, and overall model met the significance level, which was set at $\alpha = 0.05$. P-values were adjusted for the False Discovery Rate (FDR) using the approach in (Benjamini & Hochberg, 1995). For whole-brain and network- level models, FDR corrections were made across properties within each network (or the entire connectome). For node-level models, and each topological property, FDR corrections were made across nodes within a particular network. Missing data were assumed to be missing at random. In all analyses, all participants had topological properties and signal fluctuation data (the outcomes), and time of acquisition parameters (the variables of interest). Data for most other independent variables were missing for <5 % of the cohort; pubertal stage information was missing for ~19 % of the cohort, but this parameter was only included in secondary analyses and models.

Each fMRI timing parameter of interest (the primary independent variable) was individually included in models. Then, models were augmented by including combinations of 2 or all 3 timing variables. Finally, additional sets of models also included (2-way and 3-way) interactions between these variables (i.e., time-of-day*time-of-week, time-of-day*time-of-year, time-of-week*time-of-year and time-of-day*time-of-week*time-of-year). In addition to standardized regression coefficients (when appropriate), Cohen's f and d statistics were also used to estimate effect sizes for time-of-day (continuous variable) and time of week and year (binary variables), respectively, and regression coefficients were standardized when appropriate.

An additional secondary analysis was conducted to further elucidate the time-of-day scanning effects on connectome properties. Based on the median time of scanning (rounded to 14:00), the cohort was separated into two sub-cohorts: one including participants scanned before 14:00 and the other including those scanned at or after 14:00. Then, primary analyses were repeated for each sub-cohort (these analyses focused only on the best-quality fMRI run for each participant).

A set of linear regression models was also developed to investigate associations between scan acquisition time parameters and fMRI signal variability. The absolute coefficient of dispersion was the dependent variables in these models, and the same confounders and covariates as in previous models were included. The predictors of interest were the individual fMRI timing parameters.

Finally, an analysis was conducted to assess the impact of temporal acquisition effects on correlations between brain and cognitive outcomes. Specifically, linear regression models were developed to assess the impact of including scan time-of-day, time-of-week, time-of-year as individual and combinatorial adjustments on associations between topological brain properties and cognitive performance in the NIH neurocognitive battery set of tasks of the ABCD study (Luciana et al., 2018). In these models, cognitive task scores were the dependent variables and topological properties the independent variables of interest. Models were developed and compared with versus without the inclusion of scan acquisition timing parameters.

All analyses were conducted using the software MATLAB (R2021b, Mathworks, Inc.). Figures were created with software packages MRICroGL (NITRC.org) and BrainNet Viewer (Xia et al., 2013).

3. Results

Over 50 % of participants were in pre- or early adolescence (52.7 %), had median screen time of over 17 h/week (median = 1050.0 min, IQR = 923.8 min), overall slept less than the recommended amount for optimal development (median = 8-9 h, IQR = 2 h), had median BMI = 17.5 (IQR = 4.6), and were on average active (for at least 60 min/day) 3 days/week (median = 3 days, IQR = 3 days). Participant characteristics and sample statistics are provided in Table 1. Median time-of-day of the fMRI resting-state scan was 14:00. The majority of participants were scanned during the week [$n = 2499$ (60.92 %)], and less than 40 % were scanned during the weekend [1603 (39.08 %)]. In addition, almost three quarters of participants were scanned during the school year [$n = 3059$ (74.57 %)], and about a quarter during the summer break [$n = 1043$ (25.43 %)]. Participant distributions as a function of scan time variables are shown in Fig. 1.

There were no statistical differences in scan time-of-day as a function of race ($p \geq 0.08$), ethnicity ($p = 0.79$) or sleep length (recommended vs less than recommended amount, $p = 0.31$). A statistically higher proportion of youth scanned during the week slept less than the recommended amount [1296 (51.86 %) compared to 1203 (48.14 %); $p < 0.01$], but corresponding proportions of those scanned during the weekend were statistically similar [778 (48.53 %) slept the recommended amount and 825 (51.47 %) slept less than recommended; $p = 0.10$]. Among participants scanned during the school year, a statistically higher proportion slept less than the recommended amount [1596 (52.17 %) compared to 1463 (47.83 %); $p < 0.01$). Corresponding proportions of those scanned during the summer vacation period were statistically similar [518 (49.66 %) slept the recommended amount and 525 (50.34 %) slept less than recommended; $p = 0.76$]. No other statistical differences were estimated in groups dichotomized based on fMRI acquisition time parameters ($p > 0.10$).

3.1. Correlations between time parameters and topological properties

3.1.1. Connectome-wide associations

Correlations with individual scan time parameters: At the brain-wide level, only time-of-day was significantly associated with multiple network properties. Later scanning times were associated with lower estimates of efficiency, global clustering, topological robustness and stability, and higher estimates of modularity and small-worldness ($p < 0.04$) in the brain. These associations were consistent in both rs-fMRI runs. Effect sizes were overall small (Cohen's $f < 0.10$). Model statistics are summarized in Table 2a.

Correlations with multiple scan time parameters: Separate models included pairs of parameters (i.e., additive models with time-of-day and time-of-week, time-of-day and time-of-year and time-of-week and time-of-years), and then all three parameters. These can be interpreted as examining one time parameter while controlling for the other(s). Time-of-year was consistently nonsignificant in all models with combinations that included this parameter ($p > 0.05$). In models that included time-of-day and time-of-week, both were statistically associated with multiple topological properties, but only in the larger sample corresponding to the first run. Participants measured later in the day and during the week

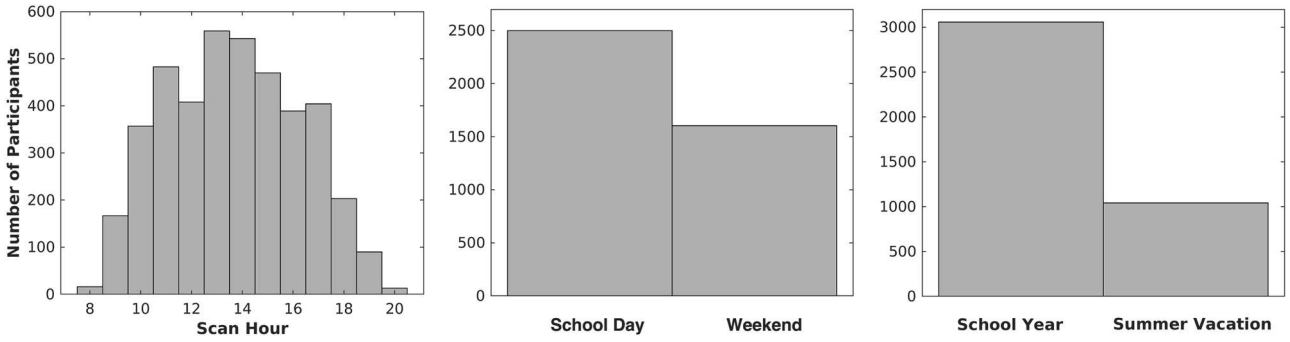

Fig. 1. Distributions of fMRI acquisition time-of-day (h), school day vs weekend, school year vs summer vacation.

Table 2a
Statistics of models testing associations between fMRI acquisition time-of-day and brain connectome-wide topological properties, for both analyzed fMRI runs. All reported p-values have been corrected for false discovery. *Nonsignificant (NS); Confidence Interval (CI)

Time of the day							
Statistic	Efficiency	Global Clustering	Median Connectivity	Modularity	Topological Robustness	Small-worldness	Topological Stability
Best-Quality fMRI Run							
Standardized Beta	-0.051	-0.035	NS*	0.064	-0.047	0.055	-0.046
95th % CI	[-0.082, -0.020]	[-0.067, -0.003)	NS	[0.033, 0.095]	[-0.079, -0.016]	[0.023, 0.087]	[-0.078, -0.015]
P-value	0.003	0.035	NS	<0.001	0.006	0.002	0.006
Cohen's f	0.051	0.032	NS	0.064	0.046	0.054	0.045
Second Best-Quality fMRI Run							
Standardized Beta	-0.065	-0.060	NS	0.061	-0.064	0.054	-0.063
95th % CI	[-0.102, -0.028]	[-0.098, -0.023]	NS	[0.024, 0.098]	[-0.101, -0.027]	[0.017, 0.091]	[-0.100, -0.025]
P-value	0.002	0.002	NS	0.002	0.002	0.005	0.002
Cohen's f	0.064	0.058	NS	0.060	0.062	0.051	0.061

had lower estimates of connectome efficiency, global clustering, topological robustness and stability, and higher estimates of modularity and small-worldness ($p < 0.03$). Similar associations for both time parameters were estimated in models that included all three time parameters ($p < 0.05$). Model statistics are summarized in Table 2b. Effect sizes were comparable for the two parameters and overall small (Cohen's $f < 0.10$, Cohen's $d < 0.24$). Two- and three-way time parameter interactions were also examined, but were all nonsignificant at this spatial scale ($p > 0.29$).

3.1.2. Network-specific associations

Correlations with individual scan time parameters: Time-of-day was correlated with multiple properties of several networks in both hemispheres, Participants scanned later in the day had lower efficiency, global clustering, within-network connectivity, topological robustness, and stability, but higher modularity estimates in bilateral central visual, dorsal attention and frontoparietal control ($p \leq 0.04$). They also had higher within-network connectivity and modularity (but no other topological differences) in left somatomotor networks, higher modularity in the bilateral salience network, lower robustness and stability only in the right salience network, higher modularity in bilateral basal ganglia, and higher topological robustness and stability in the amygdala ($p < 0.05$). Time-of-day effects were overall small (Cohen's $f < 0.10$).

Similar associations were estimated based on the second fMRI run was from all participants, along with lower efficiency, global clustering, connectivity (within- and across- network), robustness, and stability, and higher modularity in bilateral DM and limbic networks (except nonsignificant somatomotor or amygdala correlations, $p < 0.05$, Cohen's $f < 0.10$). In addition, participants scanned during the weekend had lower within-network connectivity in the left temporoparietal network and lower efficiency, global clustering, topological robustness, and stability estimates in the right hippocampus ($p < 0.05$, Cohen's $d < 0.40$). These associations were only estimated in the first fMRI run. Finally, participants scanned during the school year had lower global clustering, robustness, and stability, but higher modularity estimates in left central visual, bilateral temporoparietal, and right dorsal attention networks. They also had lower connectivity (in- and out-of-network) in the right somatomotor, dorsal attention and right temporoparietal networks, and lower out-of-network connectivity in the left temporoparietal network ($p < 0.05$, Cohen's $d < 0.82$). The estimated associations in the left visual network were consistent across both fMRI runs. Detailed model statistics for all network-specific associations with time parameters are provided in Table 3a for the first run and Supplemental Table S2 for the second run. Networks positively or negatively correlated with each time parameter are shown in Fig. 2.

Correlations with multiple scan time parameters and their interactions: Overall, the individual parameter associations did not change substantially when controlling for other temporal effects ($p < 0.05$, Cohen's $f < 0.10$). Model statistics for the first and second runs are summarized in Tables S3 and S4. Networks correlated with multiple time parameters (examining one while controlling for the other two) are shown in Fig. 2. Finally, interaction models examined associations between 2- and 3-way time parameter interactions and network-specific topological properties. Two-way interactions between time-of-day and time-of-year, time-of-week and time-of-year, and the 3-way interaction between time-of-day, time-of-week and time-of-year were consistently correlated with one (typically connectivity) or more topological properties of bilateral visual networks (central and/or peripheral; $p < 0.05$, Cohen's $f < 0.06$, Cohen's $d < 0.96$) in both runs. The interaction of time-of-day and time-of-year was also correlated with connectivity (within and across networks) of the right dorsal attention network and multiple properties of the left dorsal attention network, but only in the second run ($p \leq 0.03$, Cohen's $f < 0.08$). The 3-way interaction between time variables was also associated with all properties (except connectivity) in the bilateral Default Mode network ($p < 0.05$, Cohen's $f < 0.10$). Across networks, when significant, 2- and 3-way interactions between time parameters

Table 2b
Statistics of models testing additive associations between combinations of fMRI acquisition time parameters (pairs and triplet) and connectome-wide topological properties for both analyzed fMRI runs. Only timing parameters with significant associations are reported. All reported p-values have been corrected for false discovery. *Nonsignificant (NS); Confidence Interval (CI).

	Statistic	Efficiency	Global Clustering	Median Connectivity	Modularity	Topological Robustness	Small-worldness	Topological Stability
Time-of-day and Time-of-week								
Best-Quality fMRI Run								
School day vs Weekend (*control for time of day*)	Cohen's f	0.061	0.044	NS	0.072	0.057	0.062	0.056
	Beta	-0.040	-0.046	NS	0.037	-0.045	0.037	-0.045
	95th % CI	[-0.072, -0.008]	[-0.079, -0.013]	NS	[0.005, 0.069]	[-0.078, -0.013]	[0.005, 0.070]	[-0.078, -0.013]
	P-value	0.025	0.015	NS	0.029	0.015	0.029	0.015
	Cohen's d	0.125	0.233	NS	0.083	0.183	0.151	0.186
Second Best-Quality fMRI Run								
Time of day (*control for time of week)*	Standardized Beta	-0.069	-0.066	NS	0.066	-0.071	0.061	-0.070
	95th % CI	[-0.108, -0.030]	[-0.105, -0.027]	NS	[0.028, 0.105]	[-0.110, -0.032]	[0.022, 0.100]	[-0.109, -0.031]
	P-value	0.001	0.001	NS	0.001	0.001	0.003	0.001
	Cohen's f	0.065	0.061	NS	0.062	0.066	0.056	0.065
Time-of-day and Time-of-year								
Best-Quality fMRI Run								
Time of day (*control for time of year)*	Standardized Beta	-0.049	NS	NS	0.061	-0.045	0.053	-0.044
	95th % CI	[-0.080, -0.018]	NS	NS	[0.030, 0.092]	[-0.077, -0.013]	[0.021, 0.084]	[-0.076, -0.012]
	P-value	0.005	NS	NS	0.001	0.009	0.004	0.009
	Cohen's f	0.048	NS	NS	0.061	0.043	0.051	0.042
Second Best-Quality fMRI Run								
Time of day (*control for time of year)*	Standardized Beta	-0.064	-0.059	NS	0.061	-0.064	0.054	-0.062
	95th % CI	[-0.102, -0.027]	[-0.097, -0.022]	NS	[0.024, 0.098]	[-0.101, -0.026]	[0.017, 0.092]	[-0.100, -0.025]
	P-value	0.002	0.003	NS	0.002	0.002	0.006	0.002
	Cohen's f	0.063	0.067	NS	0.059	0.062	0.051	0.060
Time-of-day and Time-of-Week and Time-of-Year								
Best-Quality fMRI Run								
Time of day (*control for time of week and year)*	Standardized Beta	-0.060	-0.046	NS	0.071	-0.058	0.063	-0.057
	95th % CI	[-0.093, -0.028]	[-0.079, -0.012]	NS	[0.038, 0.104]	[-0.091, -0.025]	[0.029, 0.096]	[-0.090, -0.023]
	P-value	0.001	0.008	NS	<0.001	0.001	0.001	0.001
	Cohen's f	0.058	0.041	NS	0.069	0.054	0.059	0.053
School day vs Weekend (*control for time of day and year)*	Beta	-0.038	-0.044	NS	0.034	-0.043	0.034	-0.043
	95th % CI	[-0.070, -0.005]	[-0.077, -0.011]	NS	[0.001, 0.066]	[-0.076, -0.010]	[0.001, 0.067]	[-0.075, -0.010]
	P-value	0.039	0.025	NS	0.047	0.025	0.047	0.025
	Cohen's d	0.124	0.231	NS	0.082	0.183	0.150	0.186
Second Best-Quality fMRI Run								
Time of day (*control for time of week and year*)	Standardized Beta	-0.069	-0.065	NS	0.066	-0.071	0.061	-0.070
	95th % CI	[-0.108, -0.029]	[-0.105, -0.026]	NS	[0.027, 0.105]	[-0.111, -0.032]	[0.022, 0.101]	[-0.109, -0.030]
	P-value	0.001	0.002	NS	0.002	0.001	0.003	0.001
	Cohen's f	0.064	0.059	NS	0.061	0.066	0.056	0.065

were positively associated with all topological parameters except modularity, for which associations were negative. Model results are summarized in Table 3b. Networks correlated with the 3-way interaction between all time parameters are shown in Fig. 2 (bottom panel).

3.1.3. Regional (node-level) associations

Correlations between time of scan acquisition parameters and regional brain properties were also examined. Time-of-day was positively correlated with centrality (i.e., those scanned later in the day had higher centrality) of nodes in the visual (peripheral) network bilaterally ($p < 0.05$, $\beta = 0.04$ to 0.07, 95% CI = [<0.01, 0.10]), and was negatively correlated with centrality in bilateral dorsal attention networks ($p < 0.04$, $\beta = -0.07$ to -0.04, 95% CI = [-0.10, -0.01]). It was also negatively correlated with local clustering of nodes in bilateral visual (central) and dorsal attention networks ($p < 0.05$, $\beta = -0.07$ to -0.04, 95% CI = [-0.09, -0.01]), and similarly for node degree ($p < 0.05$, $\beta = -0.07$ to -0.04, 95% CI = [-0.10, -<0.01]). Positive and negative correlations with time-of-day are shown in Fig. 3.

Participants scanned during the weekend had lower regional clustering in the right somatomotor network ($p < 0.04$, $\beta = -0.06$ to -0.05, 95% CI = [-0.09, -0.02]). This correlation is shown in Fig. S1. No other associations were estimated between local topological properties and

Table 3a

Statistics of models testing associations between fMRI acquisition time parameters and individual network topological properties, for the best-quality fMRI run. All reported p-values have been corrected for false discovery. Because of the small number of parcels (nodes) corresponding to the amygdala, this structure was treated as one network comprising both hemispheres. *Nonsignificant (NS); Confidence Interval (CI).

Network	Statistic	Efficiency	Global Clustering	Median Conn. (in)	Median Conn. (out)	Modularity	Robustness	Stability
Time-of-day - Left Hemisphere								
Visual (Central)	Standardized Beta	-0.082	-0.078	-0.069	NS*	0.071	-0.080	-0.081
	95th % CI	[-0.114, -0.049]	[-0.111, -0.046]	[-0.102, -0.036]	NS	[0.039, 0.104]	[-0.113, -0.048]	[-0.114, -0.049]
	P-Value	<0.001	<0.001	<0.001	NS	<0.001	<0.001	<0.001
	Cohen's f	0.080	0.076	0.066	NS	0.070	0.078	0.079
Somatomotor	Standardized Beta	NS	NS	0.047	NS	0.041	NS	NS
	95th % CI	NS	NS	[0.015, 0.080]	NS	[0.008, 0.073]	NS	NS
	P-Value	NS	NS	0.031	NS	0.047	NS	NS
	Cohen's f	NS	NS	0.044	NS	0.037	NS	NS
Dorsal Attention	Standardized Beta	-0.076	-0.071	-0.043	-0.039	0.068	-0.072	-0.073
	95th % CI	[-0.108, -0.045]	[-0.103, -0.039]	[-0.075, -0.010]	[-0.072, -0.006]	[0.036, 0.100]	[-0.104, -0.041]	[-0.105, -0.041]
	P-Value	<0.001	<0.001	0.012	0.021	<0.001	<0.001	<0.001
	Cohen's f	0.077	0.070	0.039	0.035	0.068	0.072	0.073
Salience/Ventral Attention	Standardized Beta	NS	NS	NS	NS	0.046	NS	NS
	95th % CI	NS	NS	NS	NS	[0.014, 0.078]	NS	NS
	P-Value	NS	NS	NS	NS	0.032	NS	NS
	Cohen's f	NS	NS	NS	NS	0.044	NS	NS
Frontoparietal Control	Standardized Beta	-0.052	-0.048	NS	NS	0.044	-0.050	-0.050
	95th % CI	[-0.084, -0.020]	[-0.080, -0.016]	NS	NS	[0.013, 0.076]	[-0.082, -0.018]	[-0.081, -0.018]
	P-Value	0.005	0.006	NS	NS	0.008	0.005	0.005
	Cohen's f	0.051	0.046	NS	NS	0.042	0.049	0.048
Basal Ganglia	Standardized Beta	NS	NS	NS	NS	0.052	NS	NS
	95th % CI	NS	NS	NS	NS	[0.019, 0.084]	NS	NS
	P-Value	NS	NS	NS	NS	0.013	NS	NS
	Cohen's f	NS	NS	NS	NS	0.049	NS	NS
Time-of-day - Right Hemisphere								
Visual (Central)	Standardized Beta	-0.079	-0.072	-0.064	-0.034	0.055	-0.076	-0.077
	95th % CI	[-0.111, -0.046]	[-0.104, -0.039]	[-0.096, -0.031]	[-0.067, -0.002]	[0.023, 0.087]	[-0.108, -0.043]	[-0.109, -0.044]
	P-Value	<0.001	<0.001	<0.001	0.040	0.001	<0.001	<0.001
	Cohen's f	0.076	0.069	0.061	0.030	0.052	0.074	0.074
Dorsal Attention	Standardized Beta	-0.085	-0.071	-0.046	NS	0.077	-0.081	-0.079
	95th % CI	[-0.116, -0.054]	[-0.102, -0.039]	[-0.078, -0.013]	NS	[0.045, 0.109]	[-0.113, -0.049]	[-0.111, -0.047]
	P-Value	<0.001	<0.001	0.007	NS	<0.001	<0.001	<0.001
	Cohen's f	0.087	0.070	0.043	NS	0.077	0.081	0.079
Salience/Ventral Attention	Standardized Beta	NS	NS	NS	NS	0.052	-0.038	-0.038
	95th % CI	NS	NS	NS	NS	[0.020, 0.084]	[-0.069, -0.006]	[-0.069, -0.006]
	P-Value	NS	NS	NS	NS	0.010	0.046	0.046
	Cohen's f	NS	NS	NS	NS	0.052	0.035	0.035
Frontoparietal Control	Standardized Beta	-0.057	-0.051	NS	NS	0.039	-0.044	-0.042
	95th % CI	[-0.089, -0.026]	[-0.083, -0.019]	NS	NS	[0.007, 0.070]	[-0.076, -0.012]	[-0.076, -0.012]
	P-Value	0.003	0.006	NS	NS	0.023	0.016	0.017
	Cohen's f	0.056	0.050	NS	NS	0.036	0.072	0.040
Basal Ganglia	Standardized Beta	NS	NS	NS	NS	0.054	NS	NS
	95th % CI	NS	NS	NS	NS	[0.022, 0.087]	NS	NS
	P-Value	NS	NS	NS	NS	0.007	NS	NS
	Cohen's f	NS	NS	NS	NS	0.052	NS	NS
Time-of-day - Other Networks								
Amygdala	Standardized Beta	NS	NS	NS	NS	NS	0.048	0.053
	95th % CI	NS	NS	NS	NS	NS	[0.008, 0.088]	[0.013, 0.093]

(*continued on next page*)

Table 3a (*continued*)

Network	Statistic	Efficiency	Global Clustering	Median Conn. (in)	Median Conn. (out)	Modularity	Robustness	Stability
	P-Value	NS	NS	NS	NS	NS	0.041	0.032
	Cohen's f	NS	NS	NS	NS	NS	0.044	0.049
Time-of-Week - Left Hemisphere								
Temporo- parietal	Standardized Beta	NS	NS	-0.045	NS	NS	NS	NS
	95th % CI	NS	NS	[-0.077, -0.012]	NS	NS	NS	NS
	P-Value	NS	NS	0.047	NS	NS	NS	NS
	Cohen's d	NS	NS	0.397	NS	NS	NS	NS
Time-of-Week - Right Hemisphere								
Hippocampus	Standardized Beta	-0.060	-0.055	NS	NS	NS	-0.058	-0.053
	95th % CI	[-0.101, -0.019]	[-0.096, -0.014]	NS	NS	NS	[-0.100, -0.017]	[-0.095, -0.012]
	P-Value	0.020	0.021	NS	NS	NS	0.020	0.021
	Cohen's d	0.293	0.310	NS	NS	NS	0.311	0.341
Time-of-year - Left Hemisphere								
Visual (Central)	Standardized Beta	NS	0.037	NS	NS	-0.039	0.044	0.042
	95th % CI	NS	[0.005, 0.070]	NS	NS	[-0.071, -0.007]	[0.012, 0.076]	[0.010, 0.074]
	P-Value	NS	0.040	NS	NS	0.037	0.037	0.037
	Cohen's d	NS	0.545	NS	NS	0.509	0.605	0.572
Temporo- parietal	Standardized Beta	0.049	0.038	NS	0.040	-0.038	0.055	0.053
	95th % CI	[0.017, 0.081]	[0.005, 0.070]	NS	[0.007, 0.072]	[-0.071, -0.006]	[0.023, 0.087]	[0.021, 0.085]
	P-Value	0.007	0.025	NS	0.025	0.025	0.005	0.005
	Cohen's d	0.667	0.537	NS	0.361	0.577	0.714	0.705
Time-of-year - Right Hemisphere								
Somatomotor	Standardized Beta	NS	NS	0.041	0.047	NS	NS	NS
	95th % CI	NS	NS	[0.009, 0.073]	[0.015, 0.079]	NS	NS	NS
	P-Value	NS	NS	0.041	0.031	NS	NS	NS
	Cohen's d	NS	NS	0.442	0.560	NS	NS	NS
Dorsal Attention	Standardized Beta	0.037	0.040	0.049	0.046	NS	0.039	0.040
	95th % CI	[0.006, 0.068]	[0.009, 0.072]	[0.017, 0.081]	[0.014, 0.078]	NS	[0.008, 0.071]	[0.009, 0.072]
	P-Value	0.023	0.019	0.018	0.018	NS	0.019	0.019
	Cohen's d	0.271	0.371	0.637	0.813	NS	0.312	0.328
Temporo- parietal	Standardized Beta	0.053	0.062	0.057	0.060	-0.034	NS	0.052
	95th % CI	[0.021, 0.085]	[0.030, 0.094]	[0.025, 0.090]	[0.028, 0.092]	[-0.067, -0.002]	NS	[0.020, 0.084]
	P-Value	0.002	0.001	0.001	0.001	0.036	NS	0.002
	Cohen's d	0.624	0.739	0.643	0.656	0.507	NS	0.654

scan acquisition time parameters. To assess reliability of the findings, analyses were repeated using the second fMRI run. Consistent negative associations between time-of-day and local properties of bilateral dorsal attention networks were estimated, as well as additional associations with centrality of nodes within bilateral limbic networks, local clustering within the bilateral DMN and right salience network, and node degree in spatially distributed brain regions ($p < 0.05$, $\beta = -0.12$ to -0.01, 95% CI = [-0.17, -<0.01]).

3.4. Sub-cohort analyses

Multiscale topological correlations with fMRI acquisition time-of-day (the time parameter most frequently correlated with multiple properties across scales and networks), were also examined in sub-cohorts of participants scanned before 14:00 (median time of scanning in the cohort) versus those scanned at or after 14:00. No statistical associations with time-of-day and whole-brain topological properties were estimated in either cohort ($p > 0.05$). At the individual network scale, time-of-day was negatively associated with global clustering in the right limbic network ($p < 0.02$, $\beta = -0.06$, 95% CI = [-0.10, -0.02]) in participants scanned prior to 14:00. In those scanned at 14:00 or later, time-of-day was negatively associated with multiple properties of the bilateral visual networks and cerebellum ($p < 0.04$, $\beta = -0.05$ to -0.06, 95% CI = [-0.10, -0.01]). At the level of individual regions, time-of-day was negatively correlated with centrality in nodes within the left dorsal attention ($p < 0.03$, $\beta = -0.10$ to -0.08, 95% CI = [-0.15, -0.02]) but only in participants scanned at 14:00 or later. Time-of-day effects were overall small (Cohen's $f < 0.10$).

3.5. Correlations between spontaneous fMRI signal fluctuations and acquisition time parameters

Associations between scan acquisition time parameters and rs-fMRI signal fluctuations were then assessed at the whole-brain, hemisphere, and network levels. There were no statistical associations between absolute coefficient of dispersion and any time parameter at the whole-brain level for either fMRI run ($p > 0.05$). At the hemisphere level, there were no significant associations between any time parameter and

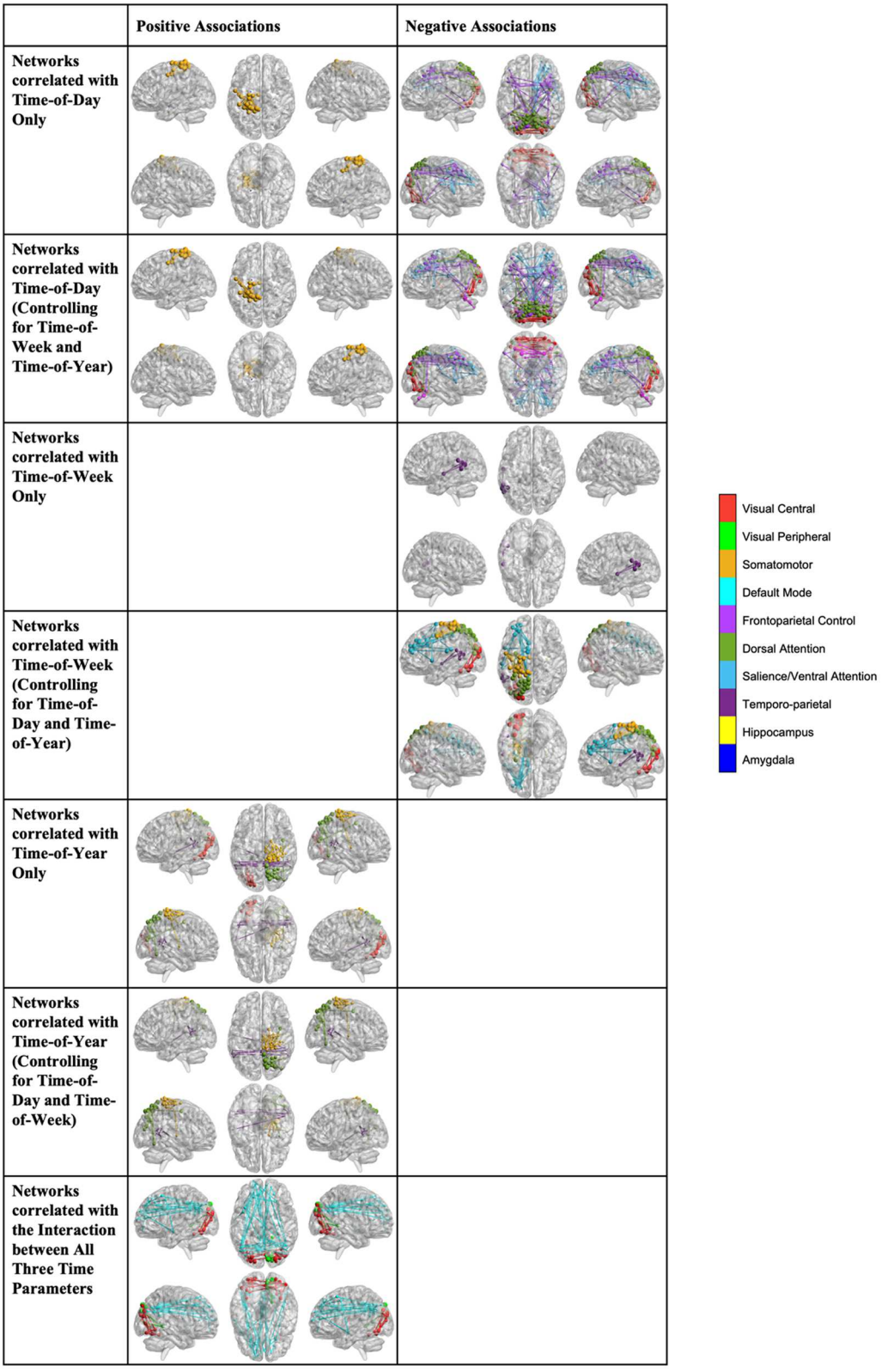

Fig. 2. Brain networks correlated with fMRI acquisition time variables. Left and right panels show positive and negative associations, respectively. Results are based on the best-quality fMRI run. Positive topological associations with time-of-week (a binary variable) implied that

and signal fluctuations for the right hemisphere. However, participants scanned later in the day had higher signal dispersion in the left hemisphere ($p = 0.04$, $\beta = 0.046$, 95% CI = [0.01, 0.08]), although only in the second fMRI run. Similar results were estimated in additive models that included time-of-day and controlled for one or both of the other two time parameters. The other two time parameters were not, however, correlated with signal fluctuation in any model ($p > 0.05$).

Table 3b
Statistics of models testing associations between 2- and 3-way interactions between acquisition time parameters and individual network topological properties, for both fMRI runs. All reported p-values have been corrected for false discovery. *Nonsignificant (NS); Confidence Interval (CI).

Network	Statistic	Efficiency	Global Clustering	Median Conn. (in)	Median Conn. (out)	Modularity	Robustness	Stability
Time-of-day * Time-of-year - Left Hemisphere								
Best-Quality fMRI Run								
Visual (Peripheral)	Standardized Beta	0.215	0.246	0.312	0.304	-0.205	0.212	0.239
	95th % CI	[0.020, 0.409]	[0.052, 0.440]	[0.118, 0.507]	[0.111, 0.498]	[-0.399, -0.012]	[0.018, 0.405]	[0.046, 0.433]
	P-Value	0.037	0.027	0.007	0.007	0.037	0.037	0.027
	Cohen's f	0.032	0.038	0.050	0.048	0.030	0.032	0.037
Second Best-Quality fMRI Run								
Visual (Peripheral)	Standardized Beta	NS*	NS	NS	0.347	NS	NS	NS
	95th % CI	NS	NS	NS	[0.117, 0.577]	NS	NS	NS
	P-Value	NS	NS	NS	0.022	NS	NS	NS
	Cohen's f	NS	NS	NS	0.054	NS	NS	NS
Dorsal Attention	Standardized Beta	NS	0.288	0.407	0.389	-0.260	0.253	0.267
	95th % CI	NS	[0.064, 0.511]	[0.180, 0.633]	[0.165, 0.613]	[-0.483, -0.038]	[0.030, 0.476]	[0.044, 0.490]
	P-Value	NS	0.027	0.002	0.002	0.030	0.030	0.030
	Cohen's f	NS	0.045	0.066	0.063	0.040	0.039	0.041
Time-of-day * Time-of-year - Right Hemisphere								
Best-Quality fMRI Run								
Visual (Peripheral)	Standardized Beta	NS*	NS	NS	0.311	NS	NS	NS
	95th % CI	NS	NS	NS	[0.116, 0.505]	NS	NS	NS
	P-Value	NS	NS	NS	0.012	NS	NS	NS
	Cohen's f	NS	NS	NS	0.049	NS	NS	NS
Second Best-Quality fMRI Run								
Visual (Central)	Standardized Beta	NS	NS	0.296	0.347	NS	NS	NS
	95th % CI	NS	NS	[0.067, 0.524]	[0.119, 0.573]	NS	NS	NS
	P-Value	NS	NS	0.039	0.020	NS	NS	NS
	Cohen's f	NS	NS	0.045	0.055	NS	NS	NS
Visual (Peripheral)	Standardized Beta	NS	NS	NS	0.346	NS	NS	NS
	95th % CI	NS	NS	NS	[0.117, 0.576]	NS	NS	NS
	P-Value	NS	NS	NS	0.022	NS	NS	NS
	Cohen's f	NS	NS	NS	0.054	NS	NS	NS
Dorsal Attention	Standardized Beta	NS	NS	0.375	0.447	NS	NS	NS
	95th % CI	NS	NS	[0.149, 0.601]	[0.220, 0.673]	NS	NS	NS
	P-Value	NS	NS	0.004	0.001	NS	NS	NS
	Cohen's f	NS	NS	0.060	0.072	NS	NS	NS
Time-of-week * Time-of-year - Left Hemisphere								
Best-Quality fMRI Run								
Visual (Central)	Standardized Beta	0.162	0.179	0.233	0.178	-0.219	0.221	0.230
	95th % CI	[0.033, 0.291]	[0.050, 0.308]	[0.102, 0.363]	[0.049, 0.307]	[-0.348, -0.091]	[0.092, 0.350]	[0.101, 0.359]
	Cohen's d	0.954	0.229	0.946	0.546	0.701	0.955	0.943
	P-Value	0.014	0.008	0.001	0.008	0.001	0.001	0.001
Time-of-week * Time-of-year - Right Hemisphere								
Visual (Central)	Standardized Beta	0.150	0.177	0.182	0.134	-0.215	0.210	0.213
	95th % CI	[0.021, 0.280]	[0.047, 0.306]	[0.052, 0.312]	[0.005, 0.264]	[-0.344, -0.086]	[0.081, 0.339]	[0.084, 0.384]
	Cohen's d	0.230	0.145	0.680	0.508	0.511	0.704	0.648
	P-Value	0.027	0.010	0.010	0.042	0.003	0.003	0.003
Time-of-day* Time-of-week * Time-of-year - Left Hemisphere								
Best-Quality fMRI Run								
Visual (Central)	Standardized Beta	0.154	0.155	0.178	0.180	-0.169	0.191	0.194

(*continued on next page*)

Table 3b (*continued*)

Network	Statistic	Efficiency	Global Clustering	Median Conn. (in)	Median Conn. (out)	Modularity	Robustness	Stability
	95th % CI	[0.039, 0.270]	[0.039, 0.270]	[0.061, 0.295]	[0.064, 0.296]	[-0.284, -0.054]	[0.076, 0.301]	[0.079, 0.310]
	Cohen's f	0.040	0.040	0.047	0.048	0.045	0.051	0.052
	P-Value	0.009	0.009	0.005	0.005	0.006	0.004	0.004
Default Mode	Standardized Beta	0.123	0.123	NS	NS	-0.170	0.161	0.161
	95th % CI	[0.009, 0.237]	[0.009, 0.238]	NS	NS	[-0.285, -0.055]	[0.046, 0.276]	[0.046, 0.276]
	Cohen's f	0.031	0.031	NS	NS	0.045	0.042	0.042
	P-Value	0.049	0.049	NS	NS	0.014	0.014	0.014
Time-of-day * Time-of-week * Time-of-year - Right Hemisphere								
Best-Quality fMRI Run								
Visual (Central)	Standardized Beta	0.154	0.159	0.154	0.150	-0.182	0.194	0.197
	95th % CI	[0.038, 0.270]	[0.043, 0.276]	[0.038, 0.271]	[0.034, 0.266]	[-0.297, -0.066]	[0.079, 0.310]	[0.081, 0.313]
	Cohen's f	0.040	0.041	0.040	0.039	0.048	0.052	0.053
	P-Value	0.011	0.011	0.011	0.011	0.005	0.004	0.004
Visual (Peripheral)	Standardized Beta	0.131	NS	NS	0.128	-0.139	0.145	0.143
	95th % CI	[0.014, 0.248]	NS	NS	[0.012, 0.244]	[-0.255, -0.024]	[0.029, 0.261]	[0.027, 0.0259]
	Cohen's f	0.032	NS	NS	0.032	0.035	0.037	0.036
	P-Value	0.044	NS	NS	0.044	0.043	0.043	0.043
Default Mode	Standardized Beta	0.128	0.129	NS	NS	-0.166	0.156	0.154
	95th % CI	[0.014, 0.263]	[0.015, 0.244]	NS	NS	[-0.282, -0.051]	[0.041, 0.271]	[0.039, 0.269]
	Cohen's f	0.033	0.033	NS	NS	0.044	0.041	0.040
	P-Value	0.039	0.039	NS	NS	0.020	0.020	0.020
Second Best-Quality fMRI Run								
Visual (Central)	Standardized Beta	NS	0.171	0.175	0.178	NS	NS	NS
	95th % CI	NS	[0.035, 0.307]	[0.038, 0.311]	[0.042, 0.314]	NS	NS	NS
	P-Value	NS	0.032	0.032	0.032	NS	NS	NS
	Cohen's f	NS	0.044	0.045	0.046	NS	NS	NS
	P-Value	0.037	0.037	0.037	0.027		0.037	0.037
	Cohen's f	0.037	0.037	0.044	0.053		0.040	0.042

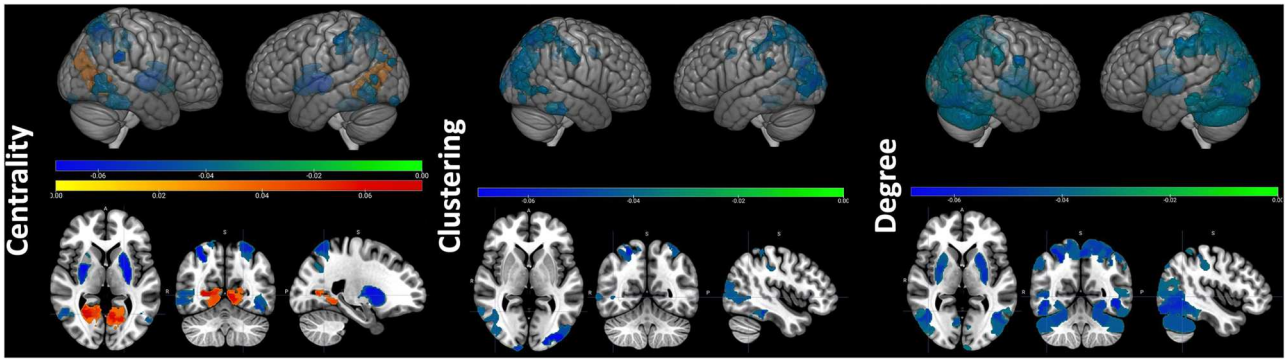

Fig. 3. Regional properties (centrality, local clustering and node degree) that are positively (orange-red) and negatively (green-blue) associated with fMRI acquisition time-of-day. Color bars represent the range of standardized regression coefficient (beta) values for the time-of-day parameter. Three-dimensional (top) and 2-dimensional (coronal, horizontal, and sagittal) views are shown.

3.6. Impact of acquisition time parameter adjustments on associations between connectome properties and cognitive task performance

Changes in estimated associations between multiscale connectome properties and performance in neurocognitive tasks performed by the ABCD participants (Luciana et al., 2018), were then examined, in models with vs withouth adjustments for acquisition time parameters. First, correlations between network topological properties and cognitive outcomes without any time parameter adjustments were investigated. Based on the first fMRI run, performance in the Dimensional Change Card Sort task was positively correlated with efficiency, global clustering, topological robustness, stability, and/or within-network connectivity of the bilateral frontoparietal and DM networks, and left dorsal attention network (only robustness and stability in the latter) ($p \leq 0.03$, $\beta = 0.04$ - 0.05, 95% CI = [0.01, 0.09]). Performance in the task was also negatively associated with modularity in the DM and right salience/ventral attention networks ($p \leq 0.03$, $\beta = -0.05$ to -0.04, 95% CI = [-0.09, -<0.01]). Similar positive and negative associations were

estimated between performance in the Oral Reading Recognition task and properties of visual and right dorsal attention networks, and between performance in the List Sorting Working Memory Task and right temporoparietal network. Negative associations were estimated between performance in the Picture Vocabulary task and within-network median connectivity of the right limbic network. Positive associations were estimated between performance in the Little Man Task and modularity of visual networks, and a negative association with global clustering in the thalamus ($p < 0.04$, $\beta = -0.07$ to -0.04, 95% CI = [-0.10, -0.01] for negative associations, $p < 0.04$, $\beta = 0.04$ - 0.06, 95% CI = [0.01, 0.09] for positive associations). Finally, negative correlations between connectivity in visual networks (both within the network and its connectivity with the rest of the brain) and performance on the Matrix Reasoning task, and positive correlations with the Cash Choice task were also estimated ($p < 0.04$, $\beta = -0.05$ to -0.04, 95% CI = [-0.08, -0.01] for negative correlations, and $\beta = 0.21$, 95% CI = [0.07, 0.35] for positive correlations). Model adjustments for individual or combinations of acquisition time parameters did not change the significance of these associations.

The analyses were repeated for the second fMRI run. Consistent with the results from the first run, associations between task performance and topological properties were estimated for the Dimensional Card Sort, Oral Reading Recognition, List Sorting Working Memory, and Little Man tasks. Additional positive associations between performance in the Pattern Comparison Processing Speed task and modularity of bilateral cerebellum and left somatomotor networks were estimated ($p < 0.04$, $\beta = 0.05$ - 0.06, 95% CI = [0.01, 0.09]). Performance in the Flanker task was also negatively correlated with modularity in the right dorsal attention network ($p = 0.05$, $\beta = -0.05$, 95% CI = [-0.09, -0.01]), and performance on the Rey Auditory Verbal Learning task with modularity of the left basal ganglia ($p = 0.03$, $\beta = -0.05$, 95% CI = [-0.09, -0.01]). Finally, performance in the Matrix Reasoning task was negatively correlated with modularity in the left dorsal attention network ($p = 0.04$, $\beta = -0.05$, 95% CI = [-0.09, -0.02]) and out-of-network connectivity in central visual networks ($p = 0.04$, $\beta = -0.04$, 95% CI = [-0.08, -0.01]. The impact of including time of acquisition adjustments in models assessing these correlations was then examined. Including time-of-day, time-of-week, or time-of-year (in models that include individual time parameters as well as all three parameters together) eliminated the association between modularity of the left somatomotor network and performance on the Pattern Comparison Processing Speed task. In addition, inclusion of all three time parameters eliminated the statistical association between out-of-network connectivity of visual networks and performance on the Matrix Reasoning task. All other significant associations remained unchanged.

4. Discussion

Cardiovascular activity, metabolic processes, body temperature and hormone (including cortisol and catecholamines) secretion, and their hourly, daily, and/or seasonal fluctuations may significantly impact blood oxygenation levels and consequently BOLD measurements in the brain. Each of these processes, and consequently cerebral hemodynamics, are also modulated by the sleep-wake cycle and circadian rhythm. Consequently, the overall timing of fMRI acquisition may affect BOLD signals in complex ways that are incompletely understood, particularly in children, and are often overlooked in neuroimaging studies.

In the developing brain, the effects of fMRI acquisition timing may be substantial, but have not been previously investigated. Specifically, in adolescence - a period of extensive and interacting neural, hormonal, metabolic, sleep, and circadian changes, these effects may be amplified, and may significantly contribute to the inherent inter-individual variability of developing brain circuits. This study has addressed this significant gap in knowledge and has systematically investigated the impact on acquisition time parameters (time-of-day, time-of-week, and time-of-year) on developing resting-state circuits across spatial scales of variability, in a large sample of over 4,000 early adolescents in the ABCD study. In addition, the confounding effects of acquisition time parameters on the relationship between brain topology and cognitive performance have also been systematically assessed.

On average, participants were scanned around 14:00, and only a small number (<5 %) were scanned before 10 am or after 6 pm. Over 60 % of participants were scanned during the week and almost 75 % during the school year. Widespread associations between time-of-day and multiscale topological properties were estimated. Overall, later acquisition times were consistently associated with lower connectome-wide and network-specific efficiency, robustness, clustering and stability, but higher values of modularity and small-worldness. Connectivity was also negatively correlated with time-of-day in specific networks. Networks consistently (across multiple fMRI runs) found to be impacted by scan time-of-day included bilateral visual, dorsal attention, salience, frontoparietal control networks and the basal ganglia, and to a lesser extent (one of the two analyzed runs) DMN and limbic networks, and amygdala. Regional properties in some of these networks were also negatively (and in a few cases positively) correlated with scan time-of-day. Lower regional connectedness (degree) and community structure (local clustering) in regions of the DMN, dorsal attention, limbic and/or visual networks were correlated with later times of scan. Regional (node) centrality (reflecting topological importance in the network) was lower in areas of the dorsal attention network but higher in areas of the peripheral visual network.

Together, our findings suggest that the time of fMRI scan plays an important role on estimates of topological organization of resting-state brain circuits, across spatial scales. They also are in agreement with those of prior studies in adults, which have reported that functional connectivity in DMN, medial temporal lobe, posterior cingulate and medial prefrontal cortex decreases throughout the day (Blautzik et al., 2013, Shannon et al., 2013, Hodkinson et al., 2014, Facer-Childs et al., 2019, Orban et al., 2020). Although our estimated time-of-day effects were relatively small, they were overall consistent across fMRI runs - indicating reliability, even after adjusting for confounding effects of sleep patterns, screen time, BMI and other participant data.

When multiscale topological properties were examined separately in subcohorts dichotomized based on time of scan (earlier than 14:00 vs 14:00 or later), fewer but consistently significant correlations between topological properties and time of scan were estimated. In addition, time of scan was correlated with properties of distinct networks and regions in the two subcohorts. In participants who were measured earlier in the day (before 14:00), later scan times were correlated with lower global clustering in the right limbic network. In those scanned in the afternoon (at or after 14:00), later scan times were correlated with multiple properties of visual networks and the cerebellum., and local properties of the dorsal attention network.

Differences in networks and regions impacted by time of scan may be associated with underlying metabolic, hormonal and cardiovascular changes throughout the day. Glucose, energy expenditure, cortisol, catecholamines and also autonomic function have circadian rhythms with peaks in the morning (Poggiogalle et al., 2018; Thossar et al., 2018). Although the entire brain may be affected by these changes, there may also be specific functional networks (e.g. limbic and/or attention) that may be differentially modulated by morning to early afternoon vs afternoon to evening scans. Chronotype differences may also partly explain differences in topological properties as a function of time of scan (Blautzik et al., 2013).

Topological correlates of scan time-of-week and time-of-year were less extensive at the whole-brain scale. However, participants scanned during the weekend had lower connectome efficiency, topological robustness and stability, and higher modularity and small-worldness than those scanned during the week. These differences were further examined at finer spatial scales. At the network level, participants scanned during the weekend had lower within-network connectivity in

the left temporoparietal network and multiple negatively affected properties in the right hippocampus, which is part of the DMN. It is possible that social jet lag (inconsistent sleep timing between weekdays and weekend), which has been associated with lower resting-state connectivity in the DMN (Zhang et al., 2020), may be one of the underlying mechanisms giving rise to these differences. However, its role could not be directly investigated in this study, since related data were not available at the ABCD baseline. Finally, lower local community structure (spatial clustering) in the somatomotor network was estimated in those scanned during the weekend compared to weekdays. This difference could be associated with being in a different global physiological state during the weekend, for example more relaxed (Al Zoubi et al., 2021), and/or with differences in sleep quality (Brooks et al., 2022).

Although there were no brain-wide effects of scan time-of-year, a number of network-specific differences were also identified between participants scanned during the school year vs school vacation. Lower global clustering, robustness and stability, in visual, temporoparietal and dorsal attention networks, and lower connectivity in right somatomotor, dorsal attention, and temporoparietal networks were estimated in those scanned during the school year. The visual network associations were consistent across runs. A statistically higher number of participants scanned during the school year slept less than the recommended amount, which could partly explain lower topological properties' values in this subcohort. However, previous work examining seasonal variations in brain activity and cognitive performance has shown that at least for some cognitive processes, brain activity in specific brain regions peaks in the summer months (Meyer et al., 2016), which would partly explain the higher topological properties' values in those scanned during the summer.

The study also examined interactions between scan time parameters. Several two-way interactions but also the interaction between all three scan time parameters were positively associated with the topological parameters of visual networks. These associations were consistent across hemispheres, runs and combinations of time parameters. In addition, the interaction of time-of-day and time-of-year (i.e., being scanned during the summer vacation and earlier in the day) was positively correlated with topological properties of the right dorsal attention. Also, the interaction of time-of-day, time-of-week and time-of-year (i.e., being scanned in the summer, during the weekend and earlier in the day) was positively associated with properties of the DMN. In other words, being scanned during the weekend and summer vacation may enhance the positive effect of being scanned in the morning.

Prior work in a large adult cohort has shown that scan time parameters impact the spontaneous temporal fluctuations of BOLD activity during a scan (Vaisvilaite et al., 2022). In this study, participants scanned later in the day had higher fMRI signal fluctuations in the left hemisphere, but no other significant correlations with scan time parameters were estimated. Therefore, our findings partly disagree with those of the adult study, which did not identify significant correlations between time of scan and effective connectivity parameters, but identified correlations with signal variability. Although effectivity connectivity was not estimated in our study, extensive and consistent (across runs) associations were estimated between resting-state connectivity with scan time parameters. fMRI-based connectome studies in adults or children typically do not account for time of scan. Findings from our study and as well as prior work suggest that at least scan time-of-day may significantly contribute to inter-individual variability of topological estimates, which is amplified in children. Therefore, it is important to assess whether this omission may impact estimated associations between functional connectivity (or other topological properties) and cognitive performance, and consequently lead to incorrect inferences. We, thus, examined correlations between performance in each of the tasks in the ABCD neurocognitive battery and properties of individual networks. The majority of identified correlations between topological properties and cognitive measures were not affected by the inclusion or exclusion of scan time parameters. However, there were a few exceptions. Performance in the Matrix Reasoning task (which measures fluid reasoning, but also visuospatial ability and visual sequencing) was negatively correlated with resting-state connectivity within the visual network and connectivity between this network and the rest of the brain, i.e., higher connectivity in this network at rest was linked with lower performance in the task. Previous work has identified negative correlations between resting-state networks, including the visual network, and performance in this task (Fraenz et al., 2021). Higher connectivity at rest could imply lower flexibility of the functional neuroarchitecture to facilitate rapid recruitment of task-positive networks, particularly in tasks measuring flexibility and fluid intelligence. When all three scan time parameters were included in models, the correlation between performance in this task and connectivity between the visual network and the rest of the brain was eliminated, suggesting that scan time effects may partly explain differences in resting-state connections between this and other networks, and not performance in the task (which was performed outside of the scanner). This finding also raises the question of potentially incorrect inference when the confounding effects of scan time parameters are not accounted for. In contrast, the correlation between connectivity within the visual network and task performance was unaffected by the inclusion of scan time variables.

Modularity of bilateral cerebellar and left somatomotor networks was positively associated with performance in the Pattern Comparison Processing Speed task, which assesses processing speed and information processing. Brain network modularity has been previously correlated with both information processing and associated speed, and their cognitive correlates (Bertolero et al., 2015), but not necessarily global measures such as number and/or size of modules (Hilger et al., 2017). When models were adjusted for all three scan time parameters, the association between task performance and modularity in the left somatomotor network was no longer significant. Again, this raises the question of incorrect inference, if scan time parameters are ignored. In contrast, the correlation between modularity of the cerebellar network and task performance was unaffected by the inclusion of scan time parameters. Together, findings from these analyses suggest that despite some invariance of connectome-cognitive performance associations to scan time effects, in some cases the latter may be significant and substantially change findings and consequently inference. Therefore, it is important to account for scan time parameters, particularly time-of-day, given its extensive associations with topological parameters across networks.

Despite its many strengths, including the size of this investigation which is sufficiently large to capture the adolescent brain's circuit heterogeneity, this study also had some limitations. First, information on typical sleep habits was available, but more granular information on sleep length the night before the scan was not. Thus, it was impossible to adjust for it. However, all analyses were adjusted for typical youth sleep length reported in the Sleep Disturbance Scale for Children. In addition, measurements of other processes that would correlate with time of scan or independently impact fMRI signals, such as cardiovascular function and metabolic/hormonal variations were not available. Although it is possible to measure heart rate in the scanner, measuring metabolic and hormonal changes is much more difficult. In addition, a retrospective investigation is always limited by the scientific decisions and data collection protocol of the original study. Although the ABCD collects extensive data across multiple processes and domains, some types of data were not collected. However, a future study focusing on the smaller subset of participants with actigraphy data prior to an fMRI scan could investigate scan time effects while adjusting for sleep length before the scan and heart rate (at least patterns, if actigraphy is not collected in the scanner). Finally, effects of time-of-week and time-of-year were assessed at a coarse level, comparing participants scanned during school days vs weekend, and school year vs summer vacation. However, other unmeasured factors that could impact the week dichotomization and time-of-week effects, such as weekend academic or other activities that would require a week-like schedule. In addition, a 5-day school week was

assumed for all youth, which may not be accurate for all, given that a small group of participants were homeschooled, with potentially different schooling schedules. Finally, the dichotomization of school year vs summer vacation was based on a typical public school calendar in the area of each ABCD site. However, participants were eligible to be scanned at a site if they lived within 50 miles from it. Therefore, without school-specific calendar information, this dichotomization may be incorrect for some participants. More granular information was, however, not available. It is, therefore, possible that some of the time-of-week and time-of-year effects may be under/overestimated. In contrast, scan time-of-day was accurately recorded for each participant.

This first-of-its kind study, based on a historically large sample of over 4000 youth that captures the inherent variability of the early adolescent brain, makes a significant contribution towards improved knowledge of confounding effects of fMRI scan timing on estimates of topological properties and signal variability. It provides first evidence that scan time-of-day, time-of-week and time-of-year may have extensive effects on resting-state properties of developing connectomes, across spatial scales, likely as a result of complex daily, circadian and seasonal fluctuations of underlying processes and physiological factors that modulate intrinsic fluctuations of BOLD activity. It also highlights that time of scan has the most spatially widespread effects (and later scan times negatively affect estimates of topological properties), and impacts temporal fluctuations of fMRI signals, but potentially differently than in adults. In youth with incompletely developed brain circuits that undergo significant topological changes, particularly during periods of heightened maturation such as adolescence, the timing of fMRI scanning may play a significant role in the variability of their connectomes. The resting-state functional circuitry is considered the backbone of the brain's neuroarchitecture, and networks such as the DMN that are active at rest play a ubiquitous role in cognitive function. Scan timing may thus impact not only resting-state network topologies but their relationships with cognitive outcomes. Findings from this study suggest that, although several of these relationships may be unaffected by when the scan is performed, for some tasks ignoring the effects of scan time parameters can lead to incorrect inferences, and spurious correlations that are influenced by scan time. Our results also point to the heterogeneity but also vulnerability of incompletely maturated functional circuits in adolescence, and complex interrelated factors such as normal daily metabolic and cardiovascular variations, but also sleep length, sleepiness and fatigue that may impact their topological organization across scales. Together these findings highlight the importance of adjusting for scan time parameters in fMRI analyses at the signal, network and/or cognitive levels, in order to increase robustness, reduce variability and maximize the generalization of neuroimaging findings in pediatric studies.

CRediT authorship contribution statement

Linfeng Hu: Data curation, Formal analysis, Investigation, Software, Visualization, Writing – original draft, Writing – review & editing. **Eliot S Katz:** Conceptualization, Writing – original draft, Writing – review & editing. **Catherine Stamoulis:** Conceptualization, Funding acquisition, Investigation, Methodology, Project administration, Resources, Supervision, Writing – original draft, Writing – review & editing.

Declaration of Competing Interest

The authors declare that they have no known competing financial interests or personal relationships that could have appeared to influence the work reported in this paper.

Data availability

This study analyzed publicly available data from the ABCD study. All data are available through the National Institute of Mental Health Data Archive (NDA). https://nda.nih.gov/.

All codes associated with this study have been made publicly available:1.

Codes associated with the fMRI data analyses can be found at: https://github.com/cstamoulis1/Next-Generation-Neural-Data-Analysis-NGNDA-.2.

Codes associated with statistical analyses in this manuscript can be found at: https://github.com/cstamoulis1/fMRI-Scan-Timing.

Acknowledgements

This work is supported by the National Science Foundation, Awards 1940096, 1649865, 2116707, 2207733

Supplementary materials

Supplementary material associated with this article can be found, in the online version, at doi:10.1016/j.neuroimage.2023.120459.

References

Abrol, A., Damaraju, E., Miller, R.L., Stephen, J.M., Claus, E.D., Mayer, A.R., et al., 2017. Replicability of time-varying connectivity patterns in large resting state fMRI samples. Neuroimage 163, 160–176.

Airan, R.D., Vogelstein, J.T., Pillai, J.J., Caffo, B., Pekar, J.J., Sair, H.I., 2016. Factors affecting characterization and localization of interindividual differences in functional connectivity using MRI. Hum. Brain. Mapp. 37 (5), 1986–1997.

Al Zoubi, O., Misaki, M., Bodurka, J., Kuplicki, R., Wohlrab, C., Schoenhals, W.A., et al., 2021. Taking the body off the mind: decreased functional connectivity between somatomotor and default-mode networks following Floatation-REST. Hum. Brain Mapp. 42 (10), 3216–3227.

Anderson, K.J., Revelle, W.J., 1994. Impulsivity and time of day: is rate of change in arousal a function of impulsivity? Pers. Soc. Psychol. 67, 334–344.

Anderson, J.A., Campbell, K.L., Amer, T., Grady, C.L., Hasher, L., 2014. Timing is everything: age differences in the cognitive control network are modulated by time of day. Psychol. Aging 29 (3), 648.

Aron, A.R., Gluck, M.A., Poldrack, RA., 2006. Long-term test-retest reliability of functional MRI in a classification learning task. Neuroimage 29 (3), 1000–1006.

Assaf, M., Jagannathan, K., Calhoun, V.D., Miller, L., Stevens, M.C., Sahl, R., et al., 2010. Abnormal functional connectivity of default mode sub-networks in autism spectrum disorder patients. Neuroimage 53 (1), 247–256.

Auchter, A.M., Hernandez Mejia, M., Heyser, C.J., Shilling, P.D., Jernigan, T.L., Brown, S. A., et al., 2018. A description of the ABCD organizational structure and communication framework. Dev. Cogn. Neurosci. 32, 8–15.

Baldassarre, A., Lewis, C.M., Committeri, G., Snyder, A.Z., Romani, G.L., Corbetta, M., 2012. Individual variability in functional connectivity predicts performance of a perceptual task. Proc. Natl. Acad. Sci. USA. 109 (9), 3516. -2.

Bandettini, PA., 2012. Twenty years of functional MRI: the science and the stories. Neuroimage 62 (2), 575–588.

Barner, C., Schmid, S.R., Diekelmann, S., 2019. Time-of-day effects on prospective memory. Behav. Brain Res. 376, 112179.

Bassett, D.S., Bullmore, E., Verchinski, B.A., Mattay, V.S., Weinberger, D.R., Meyer-Lindenberg, A., 2008. Hierarchical organization of human cortical networks in health and schizophrenia. J. Neurosci. 28 (37), 9239–9248.

Benjamini, Y., Hochberg, Y., 1995. Controlling the false discovery rate: a practical and powerful approach to multiple testing. J. R. Stat. Soc. Ser. B Stat. Methodol. 57 (1), 289–300.

Bertolero, M.A., Yeo, B.T., D'Esposito, M., 2015. The modular and integrative functional architecture of the human brain. Proc. Natl. Acad. Sci. USA. 112 (49), E6798–E6807.

Birn, R.M., Diamond, J.B., Smith, M.A., Bandettini, PA., 2006. Separating respiratory-variation-related fluctuations from neuronal-activity-related fluctuations in fMRI. Neuroimage 31 (4), 1536–1548.

Birn, R.M., Molloy, E.K., Patriat, R., Parker, T., Meier, T.B., Kirk, G.R., et al., 2013. The effect of scan length on the reliability of resting-state fMRI connectivity estimates. Neuroimage 83, 550–558.

Biswal, B., Zerrin Yetkin, F., Haughton, V.M., Hyde, J.S., 1995. Functional connectivity in the motor cortex of resting human brain using echo-planar MRI. Magn. Reson. Med. 34 (4), 537–541.

Blautzik, J., Vetter, C., Peres, I., Gutyrchik, E., Keeser, D., Berman, A., et al., 2013. Classifying fMRI-derived resting-state connectivity patterns according to their daily rhythmicity. Neuroimage 71, 298–306.

Borsook, D., Becerra, L., Hargreaves, R., 2006. A role for fMRI in optimizing CNS drug development. Nat. Rev. Drug Discov. 5 (5), 411–425.

Brooks, S.J., Parks, S.M., Stamoulis, C., 2021. Widespread positive direct and indirect effects of regular physical activity on the developing functional connectome in early adolescence. Cereb. Cortex 31 (10), 4840–4852.

Brooks, S.J., Katz, E.S., Stamoulis, C., 2022. Shorter duration and lower quality sleep have widespread detrimental effects on developing functional brain networks in early adolescence. Cereb. Cortex Commun. 3 (1), tgab062.
Brooks, S.J., Smith, C., Stamoulis, C., 2023. Excess BMI in early adolescence adversely impacts maturating functional circuits supporting high-level cognition and their structural correlates. Int. J. Obes. 3, 1–6.
Calhoun, V.D., Adalı, T., 2012. Multisubject independent component analysis of fMRI: a decade of intrinsic networks, default mode, and neurodiagnostic discovery. IEEE Rev. Biomed. Eng. 5, 60–73.
Calhoun, V.D., Miller, R., Pearlson, G., Adalı, T., 2014. The chronnectome: time-varying connectivity networks as the next frontier in fMRI data discovery. Neuron 84 (2), 262–274.
Carmichael, O., Schwarz, A.J., Chatham, C.H., Scott, D., Turner, J.A., Upadhyay, J., Coimbra, A., et al., 2018. The role of fMRI in drug development. Drug Discov. Today 23 (2), 333–348.
Chase, H.W., Phillips, M.L., 2016. Elucidating neural network functional connectivity abnormalities in bipolar disorder: toward a harmonized methodological approach. Biol. Psychiatry Cogn. Neurosci. Neuroimaging 1 (3), 288–298.
Chen, C.-H., Suckling, J., Lennox, B.R., Ooi, C., Bullmore, E.T., 2011. A quantitative meta-analysis of fMRI studies in bipolar disorder. Bipolar Disord. 13, 1–15.
Chen, B., Xu, T., Zhou, C., Wang, L., Yang, N., Wang, Z., et al., 2015. Individual variability and test-retest reliability revealed by ten repeated resting-state brain scans over one month. PLoS One 10 (12), e0144963.
Chen, X., Hsu, C.F., Xu, D., Yu, J., Lei, X., 2020. Loss of frontal regulator of vigilance during sleep inertia: a simultaneous EEG-fMRI study. Hum. Brain Mapp. 41 (15), 4288–4298.
Chen D.Y., Di X., Biswal B. Neurovascular reactivity increases across development in the visual and frontal pole networks as revealed by a breath-holding task: a longitudinal fMRI study. Biorxiv 2023 [Preprint].
Cherkassky, V.L., Kana, R.K., Keller, T.A., Just, M.A., 2006. Functional connectivity in a baseline resting-state network in autism. Neuroreport 17 (16), 1687–1690.
Clark, D.B., Fisher, C.B., Bookheimer, S., Brown, S.A., Evans, J.H., Hopfer, C., et al., 2018. Biomedical ethics and clinical oversight in multisite observational neuroimaging studies with children and adolescents: the ABCD experience. Dev. Cogn. Neurosci. 32, 143–154.
Connelly, A., 1995. Ictal imaging using functional magnetic resonance. Magn. Reson. Imaging 13 (8), 1233–1237.
Cortese, S., Kelly, C., Chabernaud, C., Proal, E., Di Martino, A., Milham, M.P., et al., 2012. Toward systems neuroscience of ADHD: a meta-analysis of 55 fMRI studies. Am. J. Psychiatry 169 (10), 1038–1055.
Crowley, S.J., Acebo, C., Carskadon, MA., 2007. Sleep, circadian rhythms, and delayed phase in adolescence. Sleep Med. 8 (6), 602–612.
Curtis, B.J., Williams, P.G., Jones, C.R., Anderson, JS., 2016. Sleep duration and resting fMRI functional connectivity: examination of short sleepers with and without perceived daytime dysfunction. Brain Behav. 6 (12), e00576.
Dichter, GS., 2012. Functional magnetic resonance imaging of autism spectrum disorders. Dialogues Clin. Neurosci. 4 (3), 319–351.
Diedrichsen, J., Balsters, J.H., Flavell, J., Cussans, E., Ramnani, N., 2009. A probabilistic MR atlas of the human cerebellum. NeuroImage 46 (1), 39–46.
Dubois, J., Adolphs, R., 2016. Building a science of individual differences from fMRI. Trends Cogn. Sci. 20 (6), 425–443.
Duncan, N.W., Northoff, G., 2013. Overview of potential procedural and participant-related confounds for neuroimaging of the resting state. J. Psychiatry Neurosci. 38 (2), 84–96.
Duyn, J., 2011. Spontaneous fMRI activity during resting wakefulness and sleep. Prog. Brain Res. 193, 295–305.
Easson, A.K., McIntosh, AR., 2019. BOLD signal variability and complexity in children and adolescents with and without autism spectrum disorder. Dev. Cogn. Neurosci. 36, 100630.
Facer-Childs, E.R., Campos, B.M., Middleton, B., Skene, D.J., Bagshaw, AP., 2019. Circadian phenotype impacts the brain's resting-state functional connectivity, attentional performance, and sleepiness. Sleep 42 (5), zsz033.
Fair, D.A., Cohen, A.L., Dosenbach, N.U., Church, J.A., Miezin, F.M., Barch, D.M., et al., 2008. The maturing architecture of the brain's default network. Proc. Natl. Acad. Sci. USA. 105 (10), 4028–4032.
Farahani, V.F., Fafrowicz, M., Karwowski, W., Bohaterewicz, B., Sobczak, A.M., Ceglarek, A., et al., 2021. Identifying diurnal variability of brain connectivity patterns using graph theory. Brain Sci. 11 (1), 111.
Farahani, F.V., Karwowski, W., D'Esposito, M., Betzel, R.F., Douglas, P.K., Sobczak, A.M., et al., 2022. Diurnal variations of resting-state fMRI data: a graph-based analysis. Neuroimage 256, 119246.
Foulkes, L., Blakemore, SJ., 2018. Studying individual differences in human adolescent brain development. Nat. Neurosci. 21 (3), 315–323.
Fox, M.D., Snyder, A.Z., Vincent, J.L., Corbetta, M., Van Essen, D.C., Raichle, ME., 2005. The human brain is intrinsically organized into dynamic, anticorrelated functional networks. Proc. Natl Acad. Sci. 102 (27), 9673–9678. Jul 5.
Fraenz, C., Schlüter, C., Friedrich, P., Jung, R.E., Güntürkün, O., Genç, E., 2021. Interindividual differences in matrix reasoning are linked to functional connectivity between brain regions nominated by parieto-frontal integration theory. Intelligence 87, 101545.
Gaggero, A., Tommasi, D., 2023. Time of day and high-stake cognitive assessments. Econ. J. 133 (652), 1407–1429.
Gaggioni, G., Maquet, P., Schmidt, C., Dijk, D.J., Vandewalle, G., 2014. Neuroimaging, cognition, light and circadian rhythms. Front. Syst. Neurosci. 8, 126.
Gao, W., Elton, A., Zhu, H., Alcauter, S., Smith, J.K., Gilmore, J.H., et al., 2014. Intersubject variability of and genetic effects on the brain's functional connectivity during infancy. J. Neurosci. 34 (34), 11288–11296.
Garrett, D.D., Kovacevic, N., McIntosh, A.R., Grady, CL., 2010. Blood oxygen level-dependent signal variability is more than just noise. J. Neurosci. 30 (14), 4914–4921.
Geerligs, L., Rubinov, M., Cam-Can, H.R.N., 2015. State and trait components of functional connectivity: individual differences vary with mental state. J. Neurosci. 35 (41), 13949–13961.
Glover, G.H., 2011. Overview of functional magnetic resonance imaging. Neurosurg. Clin. 22 (2), 133–139.
Gorfine, T., Zisapel, N., 2009. Late evening brain activation patterns and their relation to the internal biological time, melatonin, and homeostatic sleep debt. Hum. Brain Mapp. 30 (2), 541–552.
Gotman, J., Kobayashi, E., Bagshaw, A.P., Bénar, C.G., Dubeau, F., 2006. Combining EEG and fMRI: a multimodal tool for epilepsy research. J. Magn. Reson. Imaging 23 (6), 906–920. An Official Journal of the International Society for Magnetic Resonance in Medicine.
Grady, C.L., Garrett, DD., 2014. Understanding variability in the BOLD signal and why it matters for aging. Brain Imaging Behav. 8 (2), 274–283.
Greicius, M.D., Krasnow, B., Reiss, A.L., Menon, V., 2003. Functional connectivity in the resting brain: a network analysis of the default mode hypothesis. Proc. Natl Acad. Sci. 100 (1), 253–258.
Greicius, M.D., Srivastava, G., Reiss, A.L., Menon, V., 2004. Default-mode network activity distinguishes Alzheimer's disease from healthy aging: evidence from functional MRI. Proc. Natl Acad. Sci. 101 (13), 4637–4642.
Hagler Jr, D.J., Hatton, S., Cornejo, M.D., Makowski, C., Fair, D.A., Dick, A.S., et al., 2019. Image processing and analysis methods for the adolescent brain cognitive development study. Neuroimage 202, 116091.
Hernandez, L.M., Rudie, J.D., Green, S.A., Bookheimer, S., Dapretto, M., 2015. Neural signatures of autism spectrum disorders: insights into brain network dynamics. Neuropsychopharmacology 40 (1), 171–189.
Herting, M.M., Gautam, P., Chen, Z., Mezher, A., Vetter, NC., 2018. Test-retest reliability of longitudinal task-based fMRI: implications for developmental studies. Dev. Cogn. Neurosci. 33, 17–26.
Hilger, K., Ekman, M., Fiebach, C.J., Basten, U., 2017. Intelligence is associated with the modular structure of intrinsic brain networks. Sci. Rep. 7 (1), 16088.
Hodkinson, D.J., O'daly, O., Zunszain, P.A., Pariante, C.M., Lazurenko, V., Zelaya, F.O., et al., 2014. Circadian and homeostatic modulation of functional connectivity and regional cerebral blood flow in humans under normal entrained conditions. J. Cereb. Blood Flow Metab. 34 (9), 1493–1499.
Huettel, SA., 2012. Event-related fMRI in cognition. Neuroimage 62 (2), 1152–1156. Aug 15.
Itahashi, T., Yamada, T., Watanabe, H., Nakamura, M., Jimbo, D., Shioda, S., et al., 2014. Altered network topologies and hub organization in adults with autism: a resting-state fMRI study. PLoS One 9 (4), e94115.
Jezzard, P., Buxton, RB., 2006. The clinical potential of functional magnetic resonance imaging. J. Magn. Reson. Imaging 23 (6), 787–793. An Official Journal of the International Society for Magnetic Resonance in Medicine.
Jewett, M.E., Wyatt, J.K., Ritz-De, C.A., Khalsa, S.B., Dijk, D.J., Czeisler, CA., 1999. Time course of sleep inertia dissipation in human performance and alertness. J. Sleep. Res. 8 (1), 1–8.
Jiang, C., Yi, L., Su, S., Shi, C., Long, X., Xie, G., et al., 2016. Diurnal variations in neural activity of healthy human brain decoded with resting-state blood oxygen level dependent fMRI. Front. Hum. Neurosci. 10, 634.
Killgore, W.D., Vanuk, J.R., Knight, S.A., Markowski, S.M., Pisner, D., Shane, B., et al., 2015. Daytime sleepiness is associated with altered resting thalamocortical connectivity. Neuroreport 26 (13), 779–784.
Konrad, K., Eickhoff, SB., 2010. Is the ADHD brain wired differently? A review on structural and functional connectivity in attention deficit hyperactivity disorder. Hum. Brain Mapp. 31 (6), 904–916.
Kwong, K.K., Belliveau, J.W., Chesler, D.A., Goldberg, I.E., Weisskoff, R.M., Poncelet, B. P., et al., 1992. Dynamic magnetic resonance imaging of human brain activity during primary sensory stimulation. Proc. Natl Acad. Sci. 89 (12), 5675–5679.
Liao, X., Cao, M., Xia, M., He, Y., 2017. Individual differences and time-varying features of modular brain architecture. Neuroimage 152, 94–107.
Liégeois, F., Connelly, A., Cross, J.H., Boyd, S.G., Gadian, D.G., Vargha-Khadem, F., et al., 2004. Language reorganization in children with early-onset lesions of the left hemisphere: an fMRI study. Brain 127 (6), 1229–1236.
Luijten, M., Schellekens, A.F., Kühn, S., Machielse, M.W.J., Sescousse, G., 2017. Disruption of reward processing in addiction: an image-based meta-analysis of functional magnetic resonance imaging studies. JAMA Psychiatry 74 (4), 387–398.
Lynall, M.E., Bassett, D.S., Kerwin, R., McKenna, P.J., Kitzbichler, M., Muller, U., et al., 2010. Functional connectivity and brain networks in schizophrenia. J. Neurosci. 30 (28), 9477–9487.
Luciana, M., Bjork, J.M., Nagel, B.J., Barch, D.M., Gonzalez, R., Nixon, S.J., et al., 2018. Adolescent neurocognitive development and impacts of substance use: Overview of the adolescent brain cognitive development (ABCD) baseline neurocognition battery. Dev. Cogn. Neurosci. 32, 67–79.
Marek, T., Fafrowicz, M., Golonka, K., Mojsa-Kaja, J., Oginska, H., Tucholska, K., et al., 2010. Diurnal patterns of activity of the orienting and executive attention neuronal networks in subjects performing a Stroop-like task: a functional magnetic resonance imaging study. Chronobiol. Int. 27 (5), 945–958.
May, C.P., Hasher, L., 1998. Synchrony effects in inhibitory control over thought and action. J. Exp. Psychol. Hum. Percept. Perform. 24 (2), 363.

May, C.P., Hasher, L., Foon, N., 2005. Implicit memory, age, and time of day: paradoxical priming effects. Psychol. Sci. 16, 96–100.
Matthews, P., Honey, G., Bullmore, ED., 2006. Applications of fMRI in translational medicine and clinical practice. Nat. Rev. Neurosci. 7, 732–744.
McGonigle, D.J., Howseman, A.M., Athwal, B.S., Friston, K.J., Frackowiak, R.S., Holmes, AP., 2000. Variability in fMRI: an examination of intersession differences. Neuroimage 11 (6), 708–734. Pt 1.
McIntosh, A.R., Kovacevic, N., Lippe, S., Garrett, D., Grady, C., Jirsa, V., 2010. The development of a noisy brain. Arch. Ital. Biol. 148 (3), 323–337.
Meyer, C., Muto, V., Jaspar, M., Kussé, C., Lambot, E., Chellappa, S.L., et al., 2016. Seasonality in human cognitive brain responses. Proc. Natl Acad. Sci. 113 (11), 3066–3071.
Monk, C.S., Peltier, S.J., Wiggins, J.L., Weng, S.J., Carrasco, M., Risi, S., et al., 2009. Abnormalities of intrinsic functional connectivity in autism spectrum disorders. Neuroimage 47 (2), 764–772.
Mueller, S., Wang, D., Fox, M.D., Yeo, B.T., Sepulcre, J., Sabuncu, M.R., et al., 2012. Individual variability in functional connectivity architecture of the human brain. Neuron 77 (3), 586–595.
Müller, R.A., Shih, P., Keehn, B., Deyoe, J.R., Leyden, K.M., Shukla, DK., 2011. Underconnected, but how? A survey of functional connectivity MRI studies in autism spectrum disorders. Cereb. Cortex 21 (10), 2233–2243.
Murphy, K., Birn, R.M., Bandettini, PA., 2013. Resting-state fMRI confounds and cleanup. Neuroimage 80, 349–359.
Nathan, P.J., Bakker, G., 2021. Lessons learned from using fMRI in the early clinical development of a mu-opioid receptor antagonist for disorders of compulsive consumption. Psychopharmacology (Berl.) 238 (5), 1255–1263.
National Institute of Mental Health Data Archive (NDA) (2023). https://nda.nih.gov/.
Next-Generation Neural Data Analysis (NGNDA) platform. 2021. Available at: https://github.com/cstamoulis1/Next-Generation-Neur-al-Data-Analysis-NGNDA.
Ogawa, S., Tank, D.W., Menon, R., Ellermann, J.M., Kim, S.G., Merkle, H., et al., 1992. Intrinsic signal changes accompanying sensory stimulation: functional brain mapping with magnetic resonance imaging. Proc. Natl Acad. Sci. 89 (13), 5951–5955.
Orban, C., Kong, R., Li, J., Chee, M.W., Yeo, BT., 2020. Time of day is associated with paradoxical reductions in global signal fluctuation and functional connectivity. PLoS Biol. 18 (2), e3000602.
Park, B., Kim, J.I., Lee, D., Jeong, S.O., Lee, J.D., Park, HJ., 2012. Are brain networks stable during a 24-hour period? Neuroimage 59 (1), 456–466.
Patriat, R., Molloy, E.K., Meier, T.B., Kirk, G.R., Nair, V.A., Meyerand, M.E., et al., 2013. The effect of resting condition on resting-state fMRI reliability and consistency: a comparison between resting with eyes open, closed, and fixated. Neuroimage 78, 463–473.
Poggiogalle, E., Jamshed, H., Peterson, CM., 2018. Circadian regulation of glucose, lipid, and energy metabolism in humans. Metabolism 84, 11–27.
Poldrack, R.A., 2012. The future of fMRI in cognitive neuroscience. Neuroimage 62 (2), 1216–1220.
Preti, M.G., Bolton, T.A., Van De Ville, D., 2017. The dynamic functional connectome: State-of-the-art and perspectives. Neuroimage 160, 41–54.
Price, CJ., 2012. A review and synthesis of the first 20 years of PET and fMRI studies of heard speech, spoken language and reading. Neuroimage 62 (2), 816–847.
Rack-Gomer, A.L., Liu, TT., 2012. Caffeine increases the temporal variability of resting-state BOLD connectivity in the motor cortex. Neuroimage 59 (3), 2994–3002.
Raemaekers, M., du Plessis, S., Ramsey, N.F., Weusten, J.M., Vink, M., 2012. Test-retest variability underlying fMRI measurements. Neuroimage 60 (1), 717–727.
Raichle, M.E., MacLeod, A.M., Snyder, A.Z., Powers, W.J., Gusnard, D.A., Shulman, GL., 2001. A default mode of brain function. Proc. Natl Acad. Sci. 98 (2), 676–682.
Restrepo, J.G., Ott, E., Hunt, BR., 2007. Approximating the largest eigenvalue of network adjacency matrices. Phys. Rev. E 76 (5), 056119.
Rubia, K., Overmeyer, S., Taylor, E., Brammer, M., Williams, S.C., Simmons, A., et al., 1999. Hypofrontality in attention deficit hyperactivity disorder during higher-order motor control: a study with functional MRI. Am. J. Psychiatry 156 (6), 891–896.
Rubinov, M., Sporns, O., 2010. Complex network measures of brain connectivity: uses and interpretations. Neuroimage 52 (3), 1059–1069.
Schaefer, A., Kon, R., Gordon, E.M., Laumann, TO., Zuo, X.N., Holmes, A.J., et al., 2018. Local-global parcellation of the human cerebral cortex from intrinsic functional connectivity MRI. Cereb. Cortex 28 (9), 3095–3114.
Schmidt, C., Collette, F., Cajochen, C., Peigneux, P., 2007. A time to think: circadian rhythms in human cognition. Cogn. Neuropsychol. 24 (7), 755–789.
Seghier, M.L., Price, CJ., 2018. Interpreting and utilising intersubject variability in brain function. Trends Cogn. Sci. 22 (6), 517–530.
Shannon, B.J., Dosenbach, R.A., Su, Y., Vlassenko, A.G., Larson-Prior, L.J., Nolan, T.S., et al., 2013. Morning-evening variation in human brain metabolism and memory circuits. J. Neurophysiol. 109 (5), 1444–1456.
Sjuls, G.S., Specht, K., 2022. Variability in resting-state functional magnetic resonance imaging: the effect of body mass, blood pressure, hematocrit, and glycated hemoglobin on hemodynamic and neuronal parameters. Brain Connect 12 (10), 870–882.
Smith, S.M., Beckmann, C.F., Ramnani, N., Woolrich, M.W., Bannister, P.R., Jenkinson, M., et al., 2005. Variability in fMRI: a re-examination of inter-session differences. Hum. Brain Mapp. 24 (3), 248–257. Mar.
Smith, S.M., Vidaurre, D., Beckmann, C.F., Glasser, M.F., Jenkinson, M., Miller, K.L., et al., 2013. Functional connectomics from resting-state fMRI. Trends Cogn. Sci. 17 (12), 666–682.
Smith, R.J., Alipourjeddi, E., Garner, C., Maser, A.L., Shrey, D.W., Lopour, B.A., 2021. Infant functional networks are modulated by state of consciousness and circadian rhythm. Netw. Neurosci. 5 (2), 614–630.
Stam, C.J., Jones, B.F., Nolte, G., Breakspear, M., Scheltens, P., 2007. Small-world networks and functional connectivity in Alzheimer's disease. Cereb. Cortex 17 (1), 92–99.
Stoffers, D., Diaz, B.A., Chen, G., den Braber, A., van 't Ent, D., Boomsma, D.I., et al., 2015. Resting-state fMRI functional connectivity is associated with sleepiness, imagery, and discontinuity of mind. PLoS One 10 (11), e0142014.
Sun, Y., Lim, J., Kwok, KBezerianos, 2014. A, Functional cortical connectivity analysis of mental fatigue unmasks hemispheric asymmetry and changes in small-world networks. Brain Cogn. 85, 220–230.
Tian, Y., Margulies, D.S., Breakspear, M., Zalesky, A., 2020. Topographic organization of the human subcortex unveiled with functional connectivity gradients. Nat. Neurosc. 23 (11), 1421–1432.
Tsvetanov, K.A., Henson, R.N.A., Rowe, JB., 2021. Separating vascular and neuronal effects of age on fMRI BOLD signals. Philos. Trans. R. Soc. Lond. B Biol. Sci. 376 (1815), 20190631.
Vaidya, C.J., Bunge, S.A., Dudukovic, N.M., Zalecki, C.A., Elliott, G.R., Gabrieli, JD., 2005. Altered neural substrates of cognitive control in childhood ADHD: evidence from functional magnetic resonance imaging. Am. J. Psychiatry 162 (9), 1605–1613.
Vaisvilaite, L., Hushagen, V., Grønli, J., Specht, K., 2022. Time-of-day effects in resting-state functional magnetic resonance imaging: changes in effective connectivity and blood oxygenation level dependent signal. Brain Connect. 12 (6), 515–523.
Valdez, P., Ramírez, C., García, A., Talamantes, J., Armijo, P., Borrani, J., 2005. Circadian rhythms in components of attention. Biol. Rhythm Res. 36, 57–65.
Vallat, R., Meunier, D., Nicolas, A., Ruby, P., 2019. Hard to wake up? The cerebral correlates of sleep inertia assessed using combined behavioral, EEG and fMRI measures. Neuroimage 184, 266–278. Jan 1.
Van Den Heuvel, M.P., Pol, HE., 2010. Exploring the brain network: a review on resting-state fMRI functional connectivity. Eur. Neuropsychopharmacol. 20 (8), 519–534.
Van Horn, J.D., Grafton, S.T., Miller, MB., 2008. Individual variability in brain activity: a nuisance or an opportunity? Brain Imaging Behav 2 (4), 327–334.
Walter, H., Ciaramidaro, A., Adenzato, M., Vasic, N., Ardito, R.B., Erk, S., et al., 2009. Dysfunction of the social brain in schizophrenia is modulated by intention type: an fMRI study. Soc. Cognit. Affect. Neurosci. 4 (2), 166–176.
Wieth, M.B., Zacks, RT., 2011. Time of day effects on problem solving: when the non-optimal is optimal. Think. Reason. 17 (4), 387–401.
Wise, R.G., Tracey, I., 2006. The role of fMRI in drug discovery. J. Magn. Reson. Imaging 23 (6), 862–876.
Wu, J., Barahona, M., Tan, Y., Deng, H., 2009. Robustness of regular graphs based on natural connectivity. ArXiv 0912, 2144.
Wylie, G.R., Yao, B., Genova, H.M., Chen, M.H., DeLuca, J., 2020. Using functional connectivity changes associated with cognitive fatigue to delineate a fatigue network. Sci. Rep. 10 (1), 1–12.
Xia, M., Wang, J., He, Y., 2013. BrainNet viewer: a network visualization tool for human brain connectomics. PLoS One 8 (7), e68910.
Xu, Y., Cao, M., Liao, X., Xia, M., Wang, X., Jeon, T., 2019. Development and emergence of individual variability in the functional connectivity architecture of the preterm human brain. Cereb. Cortex 29 (10), 4208–4222.
Yeo, B.T., Krienen, F.M., Sepulcre, J., Sabuncu, M.R., Lashkari, D., Hollinshead, M., et al., 2011. The organization of the human cerebral cortex estimated by intrinsic functional connectivity. J. Neurophysiol. 106 (3), 1125–1165.
Yuen, N.H., Osachoff, N., Chen, JJ., 2019. Intrinsic frequencies of the resting-state fMRI signal: the frequency dependence of functional Connectivity and the effect of mode mixing. Front. Neurosci. 13, 900.
Zhang, R., Tomasi, D., Shokri-Kojori, E., Wiers, C.E., Wang, G.J., Volkow, ND., 2020. Sleep inconsistency between weekends and weekdays is associated with changes in brain function during task and rest. Sleep 43 (10), zsaa076.